Euro-TMCS II

Theory, Modelling & Computational Methods for Semiconductors

7th – 9th December 2016

Tyndall National Institute
University College Cork
Ireland

FOREWORD

Tyndall National Institute, Lee Maltings, Dyke Parade, Cork

Welcome to Euro-TMCS II: Theory, Modelling and Computational Methods for Semiconductors. Modelling, theory and the use of sophisticated computational tools can represent a substantial cost and time saving for R&D. The development of high speed computer architectures now allows the widespread use of accurate methods for calculating the structural, thermodynamic, vibrational, electronic and optical properties of semiconductors and their heterostructures.

This workshop runs for three days, with the objective of bringing together leading experts in the field of theory of group IV, III-V and wider semiconductors together with postdocs and students in their early stages who will benefit from an introduction to a very vast field at this influential point in their careers. The introductory day is a training event intended specifically for PhD students at the beginning of their studies, with high level lectures on the most used methodologies in the field. We thank the **EU MultiscaleSolar COST Action for sponsorship of 12 PhD students who submitted abstracts to the meeting and participate in the introductory day training event.**

Topics of the meeting include but are not limited to:

- Density Funtional Theory Calculations
- Tight-Binding, Pseudopotential & Effective Mass Models for Electronic Structure
- Empirical Potential Methods for Calculation of Structural
- Photonic Structures
- Optical &Transport Properties of Quantum Nanostructures including Colloidals & Nanotubes
- Plasmonics
- Electronic and Photonic
- Multiscale Approaches
- Dilute Magnetic Semiconductors
- System demands & Applications
- 2-D Systems

We are very fortunate to have also received sponsorship for Euro-TMCS II from the EU FP7 project DEEPEN. This has enabled us to provide travel support for invited speakers, as well as allowing us to set the Workshop fees at a level to encourage wide participation. We are very grateful also for sponsorship from the Institute of Physics Semiconductor Physics group, and from Failte Ireland, to support both the scientific and social activities at the Workshop.

We hope that you will enjoy the workshop and your visit to Cork and Ireland!

Eoin O'Reilly Stefan Schulz Stanko Tomic (Conference Co-Chairs)

Workshop Scientific & Programme Committee

Eoin O'Reilly (Chair),
Tyndall National Institute,
University College Cork, Ireland

Stefan Schulz (Co-Chair),
Tyndall National Institute,
University College Cork, Ireland

Stanko Tomic (Co-Chair),
Joule Physics Laboratory,
University of Salford, United Kingdom

Ben Hourahine,
University of Strathclyde,
United Kingdom

Matt Probert,
University of York,
United Kingdom

Local Organising Committee:

Janine Galvin
Eoin O'Reilly
Stefan Schulz

Programme Overview

Euro-TMCS II Theory, Modelling & Computational Methods for Semiconductors

The Conference will take place at Tyndall National Institute and University College Cork campus from 7th – 9th December.

The **Introductory Training Day** for PhD students and early career researchers will take place at the **Tyndall National Institute** (map following pages), on **Day 1**, 7th December 2016.

Registration, for those attending Day 1, will take place inside the front main entrance to Tyndall National Institute from **10:30**. The Training Day will begin in **Room A.6.G.34** at 11:30 with lectures throughout the day. **Lunch** will be provided in **Room B.0.17 Room 2**.

Day 2 & 3 will include **Invited and Contributed Talks** and will take place in the **Aula Maxima** at **University College Cork** (map following pages), on 8th and 9th December.

Invited talks are of 30 minutes duration including questions, while contributed talks are of 15 minutes duration including questions.

Registration for the Day 2 of the conference will take place at the Aula Maxima from 08:30. The day will begin with Session 1: 2-D Materials and Session 2: Nanostructures and Poster Pitches. Attendees presenting posters will be given the opportunity to outline their work in a 2 minute oral presentation. The posters will be displayed during **lunch and Poster Session** in the **Devere Hall** in the **Áras na Mac Léinn / Student Centre Building** (map following pages). Session 3: DFT & Fundamentals will follow after lunch in the **Aula Maxima** and the day will close with Session 4: New Materials. An evening networking dinner will take place on the second evening in **South's Bar at the Imperial Hotel, South Mall, Cork**.

Day 3 will begin in the **Aula Maxima** with Session 1: Hybrid Perovskites & Solar Cells. The conference will close with Session 2: Device Simulations at 12:45.

All refreshment breaks including lunch will be provided for all registered attendees on Wednesday and Thursday. If you have dietary restrictions, please make these known to the food service staff.

Directions from Cork Airport to Cork City Centre:

- Bus connections to/from the airport are provided by Bus Eireann, route No 226 to Cork Bus Station.

  Cork Bus Station is located at Parnell Place in the city centre. To get to UCC, use city buses No 205 ('CIT/Rossa Avenue') or No 208 ('Bishopstown') from the bus station or at nearby St. Patrick's Street (outside Debenham's Department Store). The bus stop code for UCC (College Road) is 241741.

- Walking from Cork Bus Station to Accommodation (Garnish House or Lancaster Lodge) is 20-25 minute walk.

- A taxi journey from Cork Airport to Accommodation (Garnish House or Lancaster Lodge) will take 10-20 minutes and will cost about €12-18.

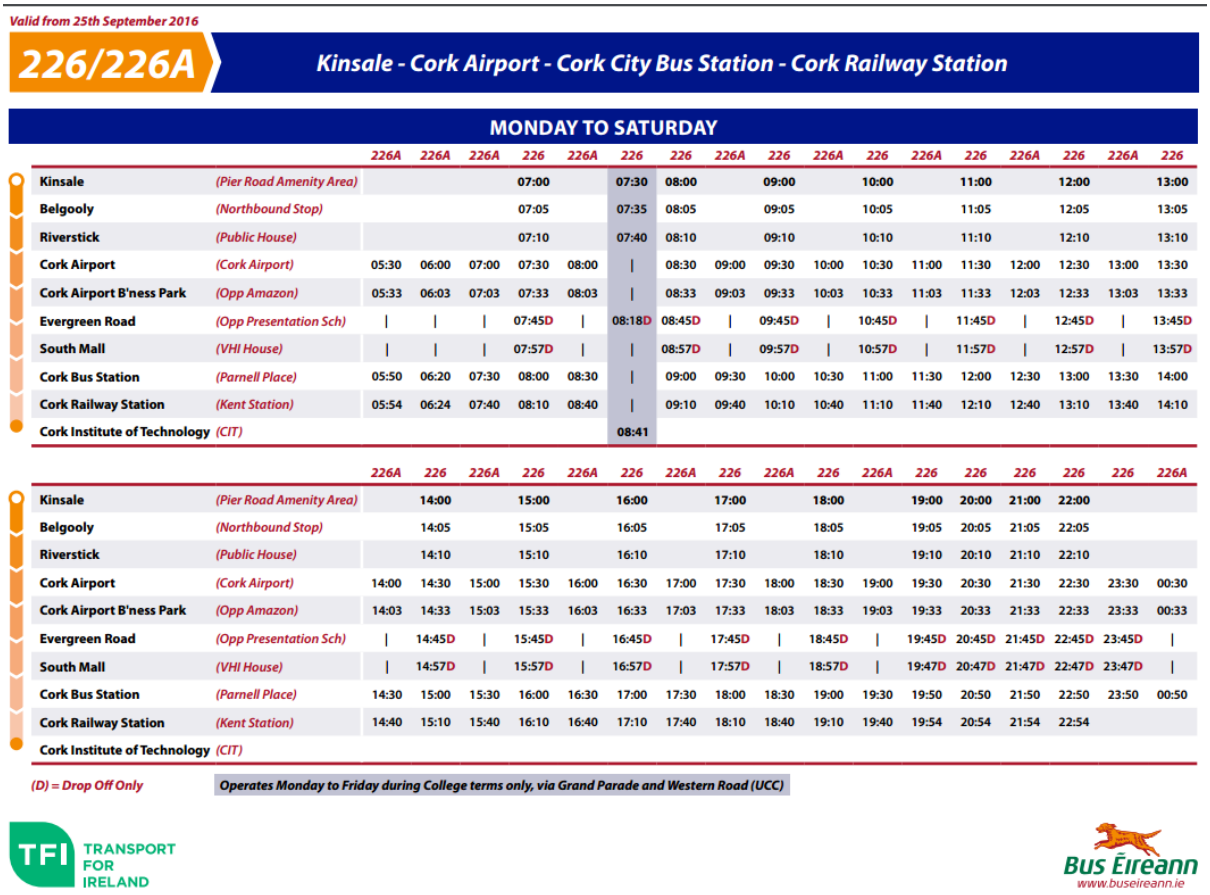

Valid from 25th September 2016

226/226A Kinsale - Cork Airport - Cork City Bus Station - Cork Railway Station

MONDAY TO SATURDAY

		226A	226A	226A	226	226A	226	226	226A	226	226A	226	226A	226	226A	226	226
Kinsale	(Pier Road Amenity Area)				07:00		07:30	08:00		09:00		10:00		11:00		12:00	13:00
Belgooly	(Northbound Stop)				07:05		07:35	08:05		09:05		10:05		11:05		12:05	13:05
Riverstick	(Public House)				07:10		07:40	08:10		09:10		10:10		11:10		12:10	13:10
Cork Airport	(Cork Airport)	05:30	06:00	07:00	07:30	08:00	|	08:30	09:00	09:30	10:00	10:30	11:00	11:30	12:00	12:30	13:00	13:30
Cork Airport B'ness Park	(Opp Amazon)	05:33	06:03	07:03	07:33	08:03	|	08:33	09:03	09:33	10:03	10:33	11:03	11:33	12:03	12:33	13:03	13:33
Evergreen Road	(Opp Presentation Sch)	|	|	|	07:45D	|	08:18D	08:45D	|	09:45D	|	10:45D	|	11:45D	|	12:45D	|	13:45D
South Mall	(VHI House)	|	|	|	07:57D	|	|	08:57D	|	09:57D	|	10:57D	|	11:57D	|	12:57D	|	13:57D
Cork Bus Station	(Parnell Place)	05:50	06:20	07:30	08:00	08:30	|	09:00	09:30	10:00	10:30	11:00	11:30	12:00	12:30	13:00	13:30	14:00
Cork Railway Station	(Kent Station)	05:54	06:24	07:40	08:10	08:40	|	09:10	09:40	10:10	10:40	11:10	11:40	12:10	12:40	13:10	13:40	14:10
Cork Institute of Technology	(CIT)						08:41											

		226A	226	226A	226	226A	226	226A	226	226A	226	226A	226	226	226	226	226	226A
Kinsale	(Pier Road Amenity Area)		14:00		15:00		16:00		17:00		18:00		19:00	20:00	21:00	22:00		
Belgooly	(Northbound Stop)		14:05		15:05		16:05		17:05		18:05		19:05	20:05	21:05	22:05		
Riverstick	(Public House)		14:10		15:10		16:10		17:10		18:10		19:10	20:10	21:10	22:10		
Cork Airport	(Cork Airport)	14:00	14:30	15:00	15:30	16:00	16:30	17:00	17:30	18:00	18:30	19:00	19:30	20:30	21:30	22:30	23:30	00:30
Cork Airport B'ness Park	(Opp Amazon)	14:03	14:33	15:03	15:33	16:03	16:33	17:03	17:33	18:03	18:33	19:03	19:33	20:33	21:33	22:33	23:33	00:33
Evergreen Road	(Opp Presentation Sch)	|	14:45D	|	15:45D	|	16:45D	|	17:45D	|	18:45D	|	19:45D	20:45D	21:45D	22:45D	23:45D	|
South Mall	(VHI House)	|	14:57D	|	15:57D	|	16:57D	|	17:57D	|	18:57D	|	19:47D	20:47D	21:47D	22:47D	23:47D	|
Cork Bus Station	(Parnell Place)	14:30	15:00	15:30	16:00	16:30	17:00	17:30	18:00	18:30	19:00	19:30	19:50	20:50	21:50	22:50	23:50	00:50
Cork Railway Station	(Kent Station)	14:40	15:10	15:40	16:10	16:40	17:10	17:40	18:10	18:40	19:10	19:40	19:54	20:54	21:54	22:54		
Cork Institute of Technology	(CIT)																	

(D) = Drop Off Only

Operates Monday to Friday during College terms only, via Grand Parade and Western Road (UCC)

TFI TRANSPORT FOR IRELAND

Bus Éireann www.buseireann.ie

Travel from Dublin Airport to Cork City Centre:

There are many direct connections to **Dublin Airport** both from North America and from Europe. There are regular express coach services from Dublin Airport to Cork (operated by Aircoach and GoBe), with a journey time of 3.5 to 4 hours. Hourly intercity train services to and from Dublin Heuston Station take between 2.5 and 3 hours.

www.aircoach.ie

www.gobe.ie

Directions from Garnish House to Tyndall National Institute:

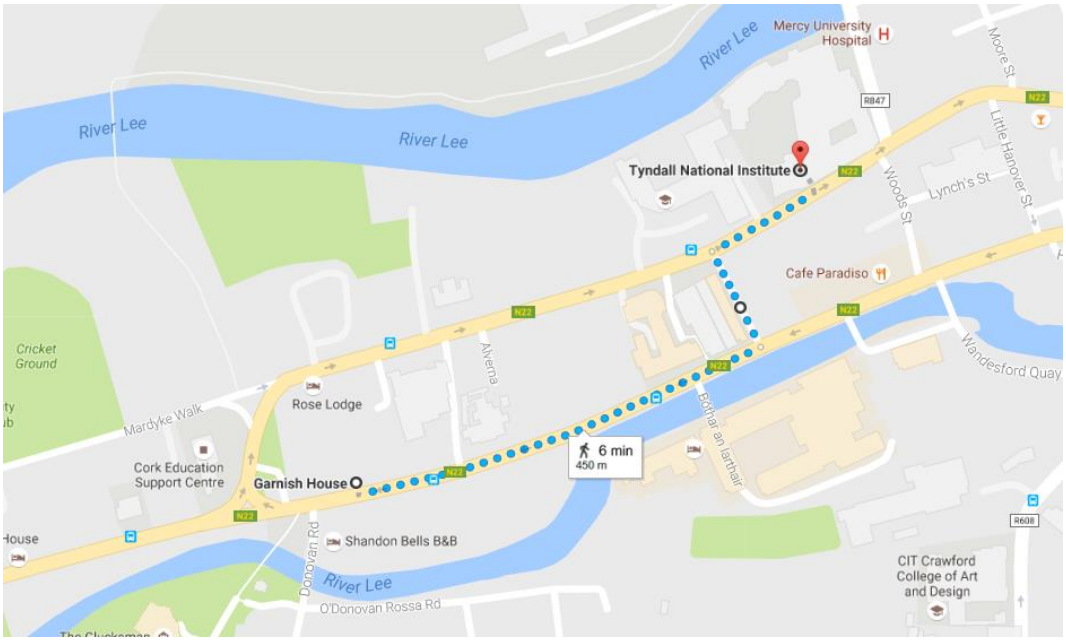

6 minute walk down Western Road. Turn left on Mardyke Street. Turn right onto Dyke Parade.

Directions from Garnish House to Aula Maxima:

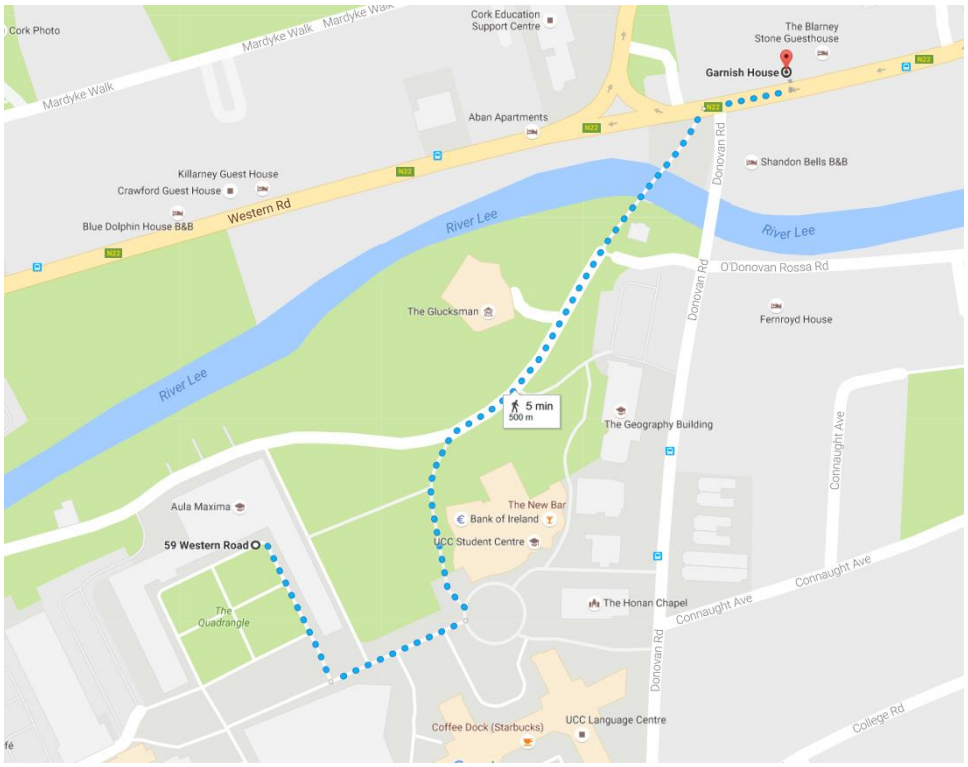

5 minute walk. Cross Western Road at traffic lights at corner of Donovan Road. Go through main black iron gates of campus. Continue up path. Veer left and up steps in front of UCC Student Centre (Bank of Ireland on map). You will see The Quadrangle buildings on the right hand side on the other side of the green. Follow walkway to the right. The Quadrangle will be on your right. Aula Maxima entrance sign posted.

Directions from Lancaster Lodge to Tyndall National Institute:

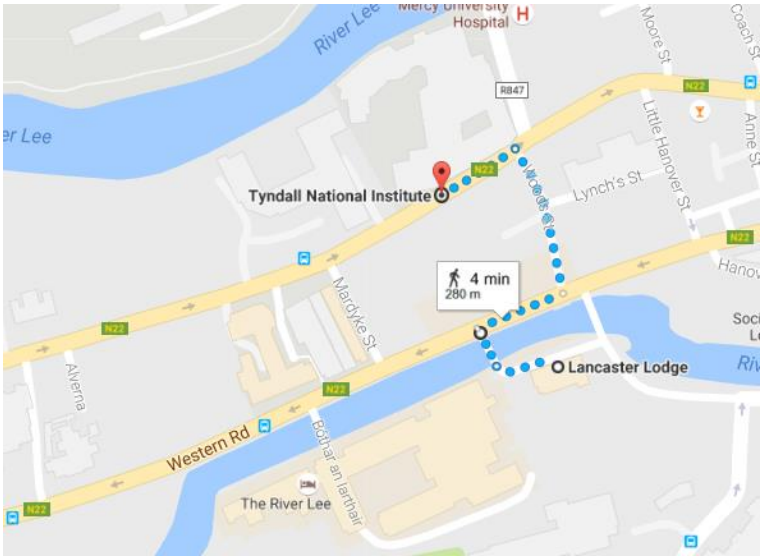

4 minute walk Lancaster Quay, over bridge. Cross Western Road at traffic lights and walk down Western Road. Turn left at Woods Street. Tyndall National Institute is building at end of street on opposite side of road.

Directions from Lancaster Lodge to Aula Maxima:

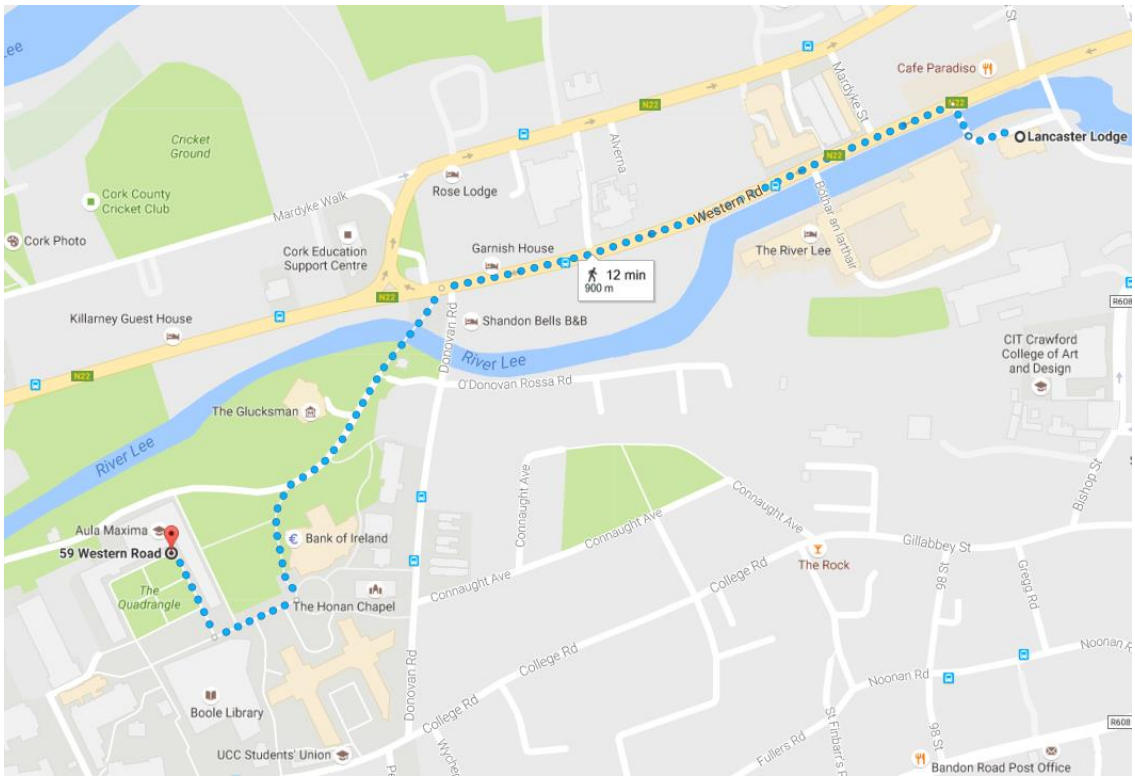

12 minute walk. Walk down Western Road. Cross Western Road at traffic lights at corner of Donovan Road. Go through main black iron gates of campus. Continue up path. Veer left and up steps in front of UCC Student Centre (Bank of Ireland on map). You will see The Quadrangle buildings on the right hand side on the other side of the green. Follow walkway to the right. The Quadrangle will be on your right. Aula Maxima entrance sign posted.

Directions from Aula Maxima to Devere Hall, Áras na Mac Léinn / Student Centre

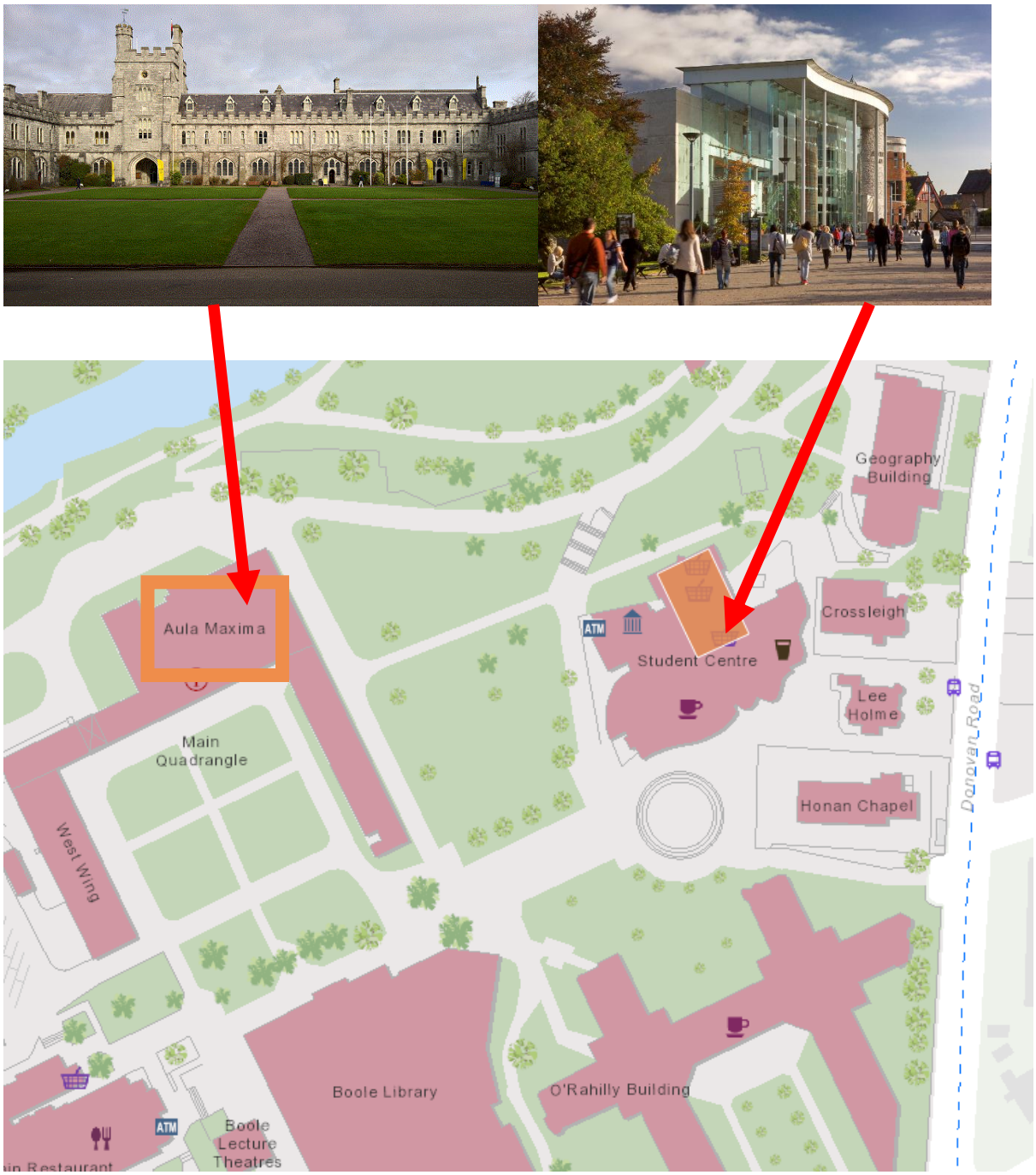

4 minute walk from Aula Maxima to Áras na Mac Léinn / Student Centre Building.

Walk across Main Quadrangle and turn left along lawn along walk way. The Student Centre Building will be immediately in front of you on your left.

The Devere Hall is located on the First Floor / Level 2 (indicated in orange on above map).

Directions from University College Cork to South's Bar at The Imperial Hotel:

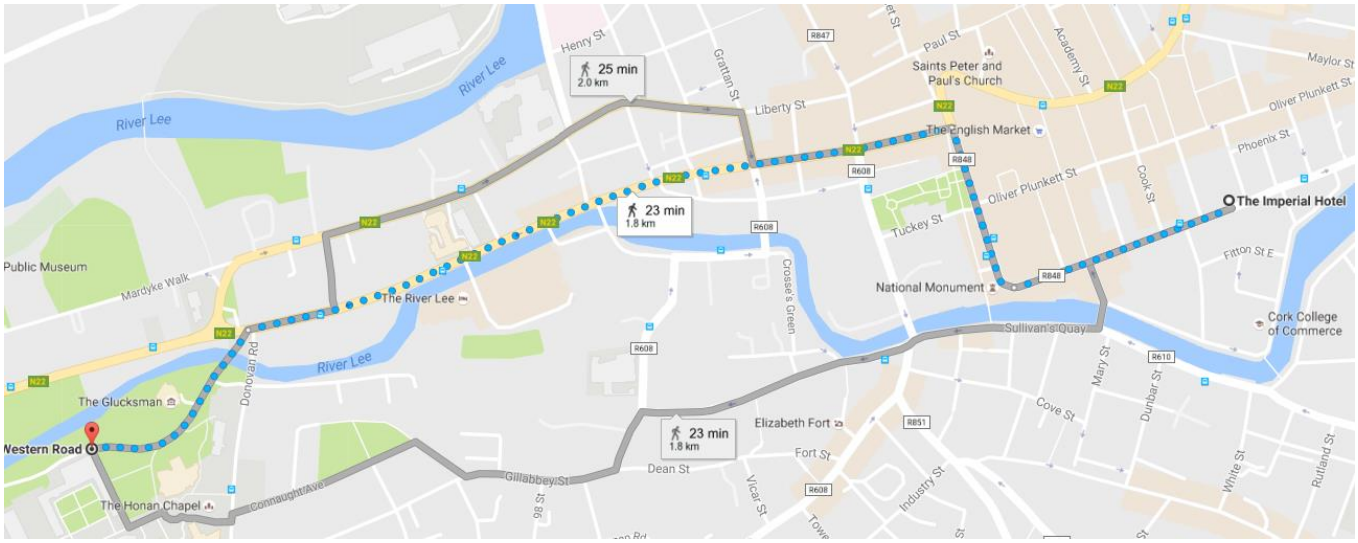

23 minute walk. Walk down Western Road to end at traffic lights. Cross over intersection and turn right along Grand Parade. Follow Grand Parade, (road turns left) which turns into South Mall. South's Bar, at The Imperial Hotel will be on the left hand side of the street.

A taxi journey from the UCC locale to South's Bar at The Imperial Hotel will take 10-12 minutes and will cost about €10-12.

List of Taxi Companies

ABC Taxis
Phone: 00 353 (0)21-4961961

Sun Cabs
Phone: 00 353 (0) 21-4292929

Satellite Cabs
Phone: 00 353 (0) 21-4808080

Cork taxis also use HAILO the Taxi App

Internet Connectivity

You may connect to Wi-Fi from the following Wireless Guest Access accounts:

Tyndall National Institute:

User Name: Euro_TMCS_II
Password: Tyndall2016

University College Cork:

User Name: ty107dec16
Password: eVMp7pe3

If you can use wireless **eduroam** please do so at University College Cork.

Day 1: 7th December 2016: Tyndall National Institute *(A.6.G.34 & B.0.17)*

Training Day Programme

10:30-11:30	Registration *(A.6.G.34)* **Registration will take place inside the front main entrance to Tyndall National Institute**
11:30-12:20	**Matt Probert** (University of York) Plane-Wave DFT and LDA
12:20-13:10	**Ben Hourahine** (University of Strathclyde) DFT-Tight-Binding Theory
13:10-14:15	Lunch *(B.0.17)*
14:15-15:05	**Stefano Sanvito** (Trinity College Dublin) Non-equilibrium Green's Function Methods
15:05-15:55	**Fabio Sacconi** (TiberLAB) Device Simulations
15:55-16:25	Coffee Break
16:25-17:15	**Jacky Even** (CNRS) Modelling of Halide Perovskites

Day 2: 8th December 2016: University College Cork (*Aula Maxima & Devere Hall*)

Regular Programme

08:30-09:00	Registration *(outside Aula Maxima)*
09:00-09:15	Welcome *(Aula Maxima)*
Session 1:	2-D Materials *(Aula Maxima)* Session Chair: **Stanko Tomic** (University of Salford)
09:15-09:45	**Thierry Amand** (INSA Toulouse) Exciton dynamics in atomically thin TMDC and their alloys: interplay between exchange and spin-orbit interaction
09:45-10:00	**Hsin Lin** (National University of Singapore) Topological Materials
10:00-10:15	**Mahdi Shirazi** (Eindhoven University of Technology) Sulfurization of 2D material: a multi-scale modelling study
10:15-10:30	**Miša Anđelković** (University of Antwerp) Large-scale conductivity calculations of (twisted) bilayer graphene
10:30-10:45	**Samuel Magorrian** (University of Manchester) Electronic and optical properties of two-dimensional InSe from DFT-parameterised tight-binding model
10:45-11:15	Coffee Break
Session 2:	Nanostructures & Poster Pitches *(Aula Maxima)* Session Chair: **Ben Hourahine** (University of Strathclyde)
11:15-11:30	**Ludwig A. Th. Greif** (Technische Universität Berlin) Modeling Energy Transfer Processes in GaN Quantum Wires

11:30-11:45 **Oliver Marquardt** (Paul-Drude-Institut für Festkörperelektronik) Influence of strain relaxation in axial $In_xGa_{1-x}N$/GaN nanowire heterostructures on their electronic properties

11:45-12:00 **Ramzi Benchamekh** (Tyndall National Institute) Impact of random alloy fluctuations on the electronic and optical properties of site-controlled (111)-oriented InGaAs/GaAs quantum dots

12:00-12:15 **Daniel Tanner** (Tyndall National Institute) Elastic properties of semiconductors beyond the limit of infinitesimal strain

12:15-12:30 **Elena Pascal** (University of Strathclyde) Theoretical model of threading dislocations strain and contrast in the scanning electron microscope images

12:30-13:00 Poster Pitches: (2 minute each)

PO1. **Pablo Palacios** (Universidad Politécnica de Madrid) Band Alignment between Intermediate Band Material and $CuAlSe_2$ and ZnS

PO2. **Joao Abreu** (Queen's University of Belfast) First principles modelling of tunnel field-effect transistors based on heterojunctions of strained Germanium/InGaAs alloy

PO3. **Abdoulwahab Adaine** (Université de Lorraine) Multivariate numerical optimization of an InGaN-based hetero junction solar cell

PO4. **Hela Boustanji** (Faculté des Sciences de Tunis) Effect of thermal annealing on the performance of type-II GaSb/GaAs quantum dots solar cell

PO5. **Silviu Bogusevschi** (Tyndall National Institute) AlGaInP-based Quantum Dot LEDs as efficient red light sources

PO6. **Saroj Kanta Patra** (Tyndall National Institute) Theoretical study of the optical properties of a-plane InGaN/GaN quantum dots

PO7. **Oliver Marquardt** (Paul-Drude-Institut für Festörperelektronik) Electronic properties of GaAs crystal phase nanostructures

PO8. **Miguel A. Caro** (Aalto University) Configurational effects on the piezoelectricity of semiconductor alloys: the case of ScAlN

PO9. **Edmond O'Halloran** (Tyndall National Institute) Direct band gaps from GeSn alloys: A hybrid functional density functional theory based analysis

PO10. **Rikmantra Basu** (National Institute of Technology Delhi) Tunnel Injection Transistor Lasers: A Group IV Material based Analysis

PO11. **Federico Iori** (Université Paris Sud) Engineering $SrTiO_3$/$LaAlO_3$ heterostructures thickness: an abinitio study

PO12. **Stephen Rhatigan** (Tyndall National Institute) Ceria-Titania Interfaces for CO_2 and Water Activation

PO13. **Luke Wilson** (Swansea University) Study of the impact of electrodes in the electron transport through Guanine and 8-oxoGuanine

PO14. **Ben Hourahine** (University of Strathclyde) Semi-emperical time-dependent DFT for plasmonic systems

PO15. **Orest Malyk** (Lviv Polytechnic National University) The local electron interaction with crystal lattice defects in cadmium telluride: ab initio approach

13:00-14:45	Lunch & Poster Session *(Devere Hall, Áras na Mac Léinn / Student Centre Building)*
Session 3:	DFT & Fundamentals *(Aula Maxima)* Session Chair: **Matt Probert** (University of York)
14:45-15:15	**Patrick Rinke** (Aalto University) Charge transfer at organic-inorganic interfaces
15:15-15:30	**Manveer Singh Munde** (University College London) Mechanism for Oxygen Vacancy Accumulation Under Electron Injection Conditions in Amorphous Silicon Oxides
15:30-15:45	**Miguel A. Caro** (Aalto University) Amorphous carbon as a versatile semiconductor material for analytical electrochemistry
15:45-16:00	**Ben Hourahine** (University of Strathclyde) Making Correlated Systems More Tractable
16:00-16:30	Coffee Break
Session 4:	New Materials *(Aula Maxima)* Session Chair: **Patrick Rinke** (Aalto University)
16:30-17:00	**Ivana Savic** (Tyndall National Institute) Modelling of the thermoelectric properties of materials near soft mode phase transitions
17:00-17:15	**Mikael Råsander** (Imperial College London) Physical properties of the wide band gap II-IV nitride $MgSiN_2$
17:15-17:30	**Laurentiu Baschir** (National Institute R&D of Optoelectronics) Surface plasmon resonance simulations in structures with chalcogenide layer
17:30-17:45	**Frank C. Maier** (University of Stuttgart) DNA sequencing using diamondoid-functionalized nanopores
19:30	Networking Dinner at South's Bar at The Imperial Hotel http://www.flynnhotels.com/Imperial_Hotel_Cork/souths-bar.html

Day 3: 9th December 2016: University College Cork *(Aula Maxima)*

Session 1:	Hybrid Perovskites & Solar Cells *(Aula Maxima)* Session Chair: **Ivana Savic** (Tyndall National Institute)
09:00-09:30	**Mark van Schilfgaarde** (King's College London) Unusual Optical Properties of MAPI
09:30-09:45	**Matko Mužević** (University of J. J. Strossmayer in Osijek) Band gap engineering in perovskites as solar cell buffer layers
09:45-10:00	**Urs Aeberhard** (Forschungszentrum Jülich) Computational challenges in the NEGF simulation of mesoscopic solar cell components
10:00-10:15	**Slobodan Čičić** (University of Salford) Heuristic modelling of multi-junction solar cells
10:15-10:30	**Philippe Czaja** (Forschungszentrum Jülich) Optoelectronic properties of a-Si:H and a-Si:H.c-Si interfaces from first principles
10:30-11:00	Coffee Break
Session 2:	Device Simulations *(Aula Maxima)* Session Chair: **Miguel A. Caro** (Aalto University)
11:00-11:30	**Yuh-Renn Wu** (National Taiwan University) Challenges in Optoelectronic Device Simulation
11:30-11:45	**Fabio Sacconi** (TiberLAB) Effects of strain distribution on the emission properties of (In,Ga)N/GaN nanowire LEDs
11:45-12:00	**Christopher A. Broderick** (University of Bristol) Theory of InGaBiAs/InP mid-infrared semiconductor lasers
12:00-12:15	**Antonio Martinez** (Swansea University) Impact of short range Coulomb repulsion on the current through a 1D Nanostructure
12:15-12:30	**Pedram Razavi** (Tyndall National Institute) Effect of alloy and dopant scattering in $In_{1-x}Ga_xAs$ nanowires
12:30-12:45	**Markus Kantner** (Weierstrass Institute for Applied Analysis and Stochastics) Multi-scale modelling and simulation of single-photon sources on a device level

Day 2

Session 1

Thursday, 8th December

09:00-10:45

2-D Materials

Exciton dynamics in atomically thin TMDC and their alloys: interplay between exchange and spin-orbit interaction

T. Amand, J. P. Echeverry, C. Robert, I.-C. Gerber, F. Cadiz, G. Wang
B. Urbaszek and X. Marie
Laboratoire de Physique et Chimie des Nano - Objets, University of Toulouse, France

Transition metal dichalcogenides (TMDCs), binary compounds of the type MX_2 (M=Mo,W; X=S,Se,Te), are 2D-semiconductors which crystallize in a honeycomb structure. In contrast to graphene, the spin-orbit interaction is strong in TMDCs, of the order of hundreds of meV in the valence band, and a few tenth of meV in the conduction band. When thinned down to one monolayer, they become direct gap semiconductors at the *K* points of the Brillouin zone edge, with chiral optical selection rules for interband transitions. Due to the confinement of the carriers within only three atomic planes, the electron-hole Coulomb interaction is strongly enhanced. The optical properties are then strongly dominated by excitonic effects[1]. The direct Coulomb interaction between the electron and the hole leads to tightly bound excitons, with binding energies larger than those of wide gap 3D-semiconductors (like Alkali-halides). As a consequence a non-hydrogenic series of bound states appears. The spin conserving dipolar optical selection rules cast the excitons into two classes: the active and the non-active ones (termed "bright" and "dark" respectively).

In this talk, we will elucidate the different contributions to the dark-bright splitting of 1s-excitons. We show using density functional theory (DFT) at the level G_0W_0 and Bethe-Salpeter (BSE) equations that both spin-orbit interaction and short-range Coulomb exchange contributions must be taken into account[2]. Two classes of materials then merge (Fig.1a): those where the Bright-dark splitting is positive (like WSe_2) and those where it is negative (like $MoSe_2$). We show that this explains the dependence of the intensity of the exciton luminescence on temperature we observed experimentally for WSe_2, $MoSe_2$, and allows for spin-orbit engineering in their alloys[3] (Fig.1b). Finally, we will evoke the role of long-range Coulomb exchange in exciton fine structure splitting, and its consequences on bright exciton spin-valley dynamics and alignment.

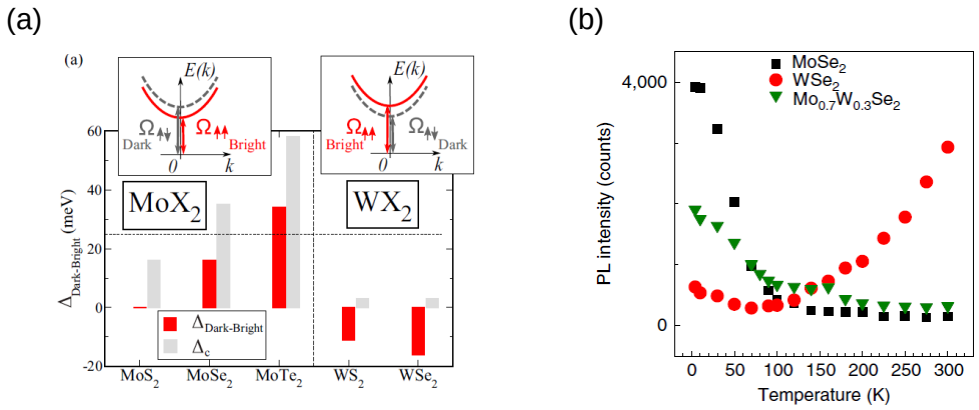

Fig.1. (a): Dark-bright exciton splitting $\Delta_{dark\text{-}Bright}$ for A_{1s}-exciton in MoX_2 et WX_2 compounds from DFT calculations at the level G_0W_0 + BSE, and contribution Δ_c corresponding to spin-orbit coupling in conduction bands. (b): Variation of the total spectrally-integrated emitted intensity of three exfoliated monolayer samples of $Mo_{1-x}W_xSe_2$ (x = 0; 0.3; 1).

[1] G. Wang *et al*., Phys. Rev. Lett. **114**, 097403 (2015)
[2] J. P. Etcheverry *et al*., Phys. Rev. B 93, 121107(R) (2016)
[3] G. Wang, *et al*., Nature Communications | 6:10110 | DOI: 10.1038/ncomms10110 | (2015)

Topological Materials

Hsin Lin
Department of Physics, National University of Singapore, Singapore 117542. Centre for Advanced 2D Materials and Graphene Research Centre, National University of Singapore, Singapore 117546.

Topological materials host various novel quantum phases of electrons which are characterized by band topology and topologically protected surface/edge states. Despite recent progress, intense world-wide research activity in search of new classes of topological materials is continuing unabated. This interest is driven by the need for materials with greater structural flexibility and tunability to enable viable applications in spintronics and quantum computing. We have used first-principles band theory computations to successfully predict many new classes of 3D topologically interesting materials, including Bi_2Se_3 series, the ternary half-Heusler compounds, $TlBiSe_2$ family, Li_2AgSb-class, and $GeBi_2Te_4$ family as well as topological crystalline insulator (TCI) SnTe family and Weyl semimetals TaAs, $SrSi_2$, (Mo,W)Te_2, Ta_3S_2, and LaAlGe family.[1,2,3,4,5] I will also highlight our recent work on 2D topological materials. These include Bi/Sb honeycombs for TCI, gated silicene for spintronics applications, and hydrogenated III-V thin films as robust topological insulators with large band gaps.[6,7,8]

[1] S M Huang et al., Nat Commun 6, 7373 (2015)
[2] S M Huang et al., PNAS 113, 1180 (2016)
[3] T R Chang et al., Nat Commun 7, 10639 (2016)
[4] G Chang et al., Science Advances 2, e1600295 (2016)
[5] G Chang et al., arXiv 1604.02124 (2016); S Y Xu et al., arXiv 1603.07318 (2016)
[6] C H Hsu et al., Scientific Reports 6, 18993 (2016)
[7] W F Tsai et al., Nat Commun 4, 1500 (2013)
[8] C Crisostomo et al., Nano Lett 15, 6568 (2015)

Sulfurization of 2D material: a multi-scale modelling study

Mahdi Shirazi, Wilhelmus M. M. Kessels, Ageeth A. Bol,
Department of applied physics, Eindhoven University of Technology, The Netherlands

Recently, the two-dimensional (2D) transition-metal dichalcogenides (TMDs) (MX_2, such as M=Mo, Ti, etc. and X=S, Se, and Te) have attracted scientific and technological interest. Unlike graphene, 2D-TMDs can exhibit metallic or semiconducting properties, depending on the transition metal or chalcogen in the crystal. The combination of an ultrathin body with semiconducting properties make 2D-TMDs key candidates for future electronic and optoelectronic nanodevice applications, To make the 2D-TMDs viable for future applications, a reliable and scalable synthesis of wafer-scale thin films with atomically controlled layers is the prerequisite. In a bottom-up synthesis, an ultra-thin film of MoO_3, is sulfurized by a gas mixture of H_2S/H_2 to MoS_2 at the relatively low temperature (< 500 K). Here, an integrated density functional theory (DFT) and kinetic Monte-Carlo calculation (KMC) modelling approach is employed to provide thermodynamic insight into the growth of the prototypical 2D material MoS_2. The DFT calculations are performed using a generalized gradient approximation (GGA) functional parametrized by Perdew, Burke, and Ernzerhof (PBE). The Vienna *ab initio* software package (VASP) is employed with the provided projector augmented wave (PAW) pseudopotential. Mo atoms are assigned a *U* parameter to correct the self-interaction error present in GGA. To treat the weakly bonded layered solids, van der Waals (vdW) interaction is applied by using the dispersion corrected DFT (optPBE-vdW functional). The detailed picture of the sulfurization mechanism, including a resolution to the reduction mechanisms of MoO_3 and the conversion into MoS_2, will be obtained. The calculated activation energies of reactions in different local chemistry, along with structural reformation, will be implemented into a 3D on-lattice (KMC). In this integrated approach (DFT+MKC), retaining the accuracy of the atomistic model in the higher-scale model leads to remarkable breakthroughs in our understanding.

Large scale conductivity calculations of (twisted) bilayer graphene

M. Anđelković, L. Covaci and F. M. Peeters
Departement Fysica, Universiteit Antwerpen, Groenenborgerlaan 171, B2020
Antwerpen, Belgium

Real space methods for calculating transport in solid state physics are of great importance, as they easily allow the inclusion of different disorder effects. A problem that can occur when using atomistic methods with realistically large devices is the complexity of the numerical approach and the availability of computational resources. We will describe a novel and highly efficient numerical approach for calculating the longitudinal and transversal DC conductivity based on the KuboBastin formula in the linear response regime, which scales linearly with the system size[1]. A great benefit of the method is the possibility for parallelization both on CPU and GPU, which greatly improves capabilities of the calculations.

We apply this method to single layer (SL), bilayer (BL) and twisted bilayer (TBL) graphene (G), the last being in our main focus. Beside the introduction of disorder, we can easily consider the effects of magnetic and/or electric fields, simply by introducing them to our tight binding model.

Interlayer coupling at small twist angles of TBLG is significant. In the presence of perpendicular electric field it induces the appearance of topologically protected helical states at domain boundaries[2]. The effects of those states in the case of TBLG on the longitudinal and transversal conductivities in the quantum Hall regime is examined. We show frequency dependent conductivity, being calculated in the same numerically efficient manner. The described method needs only the tight binding Hamiltonian matrix, and the position of atomic sites, so it can easily be used for any type of crystal structure. Also, the new approach with applied absorbing boundary conditions allows us to continuously change the magnetic field, and examine bulk properties.

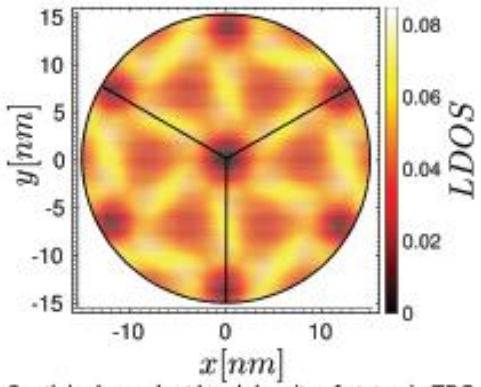

Spatialy dependent local density of states in TBG at 1° rotation angle, helical states are shown.

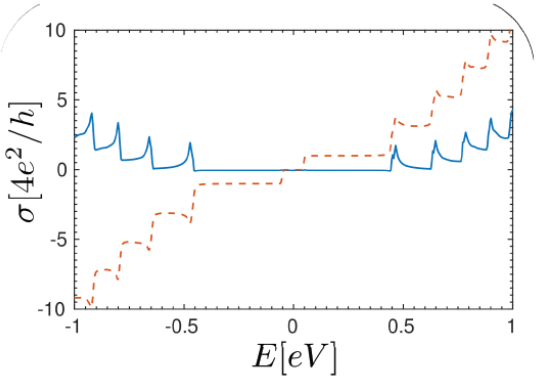

Longitudinal (solid line) and transversal (dashed line) conductivity with respect to chemical potential of TBLG in magnetic field with large rotation angle (21.79°).

[1] J.H. García, L. Covaci, and T. G. Rappoport, Phys. Rev. Lett. 114, 116602 (2015).
[2] P. SanJose and E. Prada, Phys. Rev. B 88, 121408(R) (2013).

Electronic and optical properties of two-dimensional InSe from DFT-parameterised tight-binding model

S.J. Magorrian, V. Zólyomi, and V.I. Fal'ko
National Graphene Institute, University of Manchester, United Kingdom

We present density functional theory (DFT) and a tight-binding (TB) model to describe the band structure of monolayer indium[1] and gallium[2] chalcogenides. The TB model is constructed using *s* and *p* orbitals, with parameters obtained by fitting dispersions and orbital compositions of the wavefunctions in the bands to DFT calculations, and it includes both intra- and interlayer hoppings to describe few-layer structures. The TB model was used to calculate the matrix element of the interband optical transition for in-plane polarized light, and to calculate the dependence of the corresponding lines in PL on the number of layers. The interband optical transition is suppressed in the monolayer case due to the symmetry of the bands, but is allowed for the few-layer case, with the strength increasing with the number of layers.

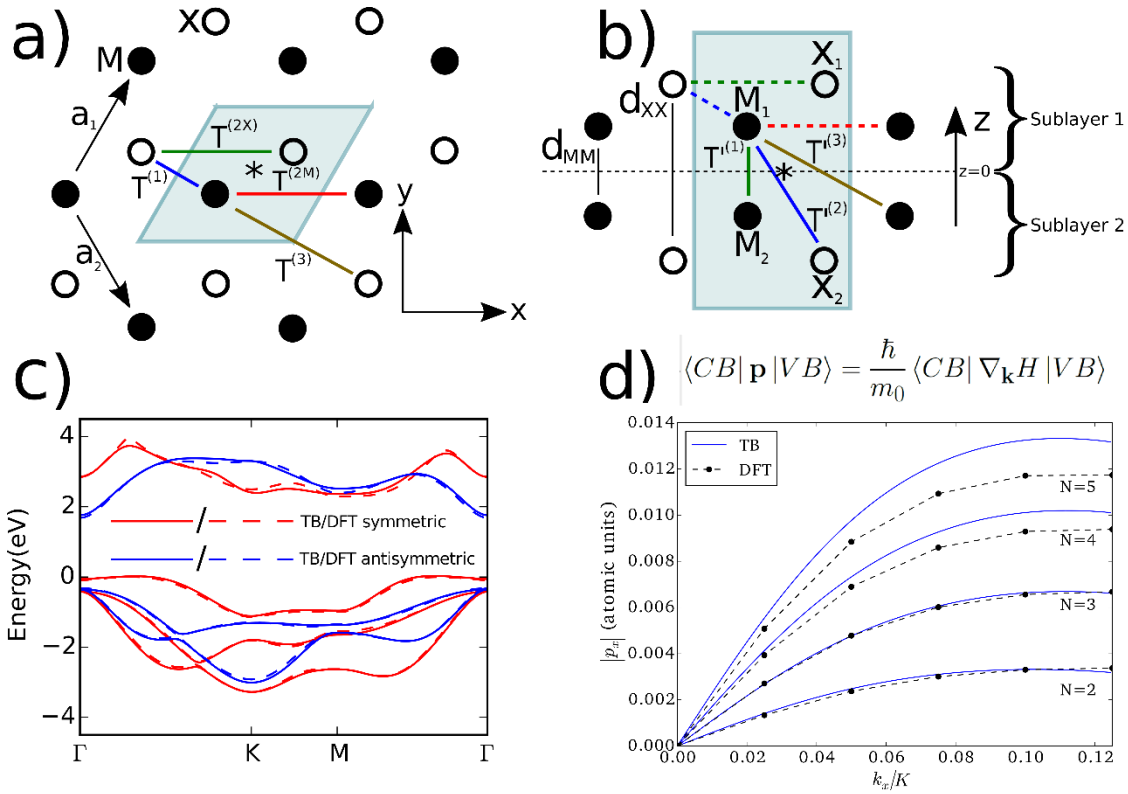

Fig.1 a) Schematic of top down view of monolayer M_2X_2 (M=In or Ga, X=Se or S) and b) side view. c) Comparison of fitted tight-binding (TB) low energy bandstructure for InSe with DFT results, line colours denote symmetry of wavefunctions under reflection about z=0. d) Interband momentum matrix elements near Γ from DFT and TB model for N-layer γ-InSe, with N up to 5 layers. The TB values are calculated from the TB Hamiltonian using the expression given.

[1] Zólyomi, V., N. D. Drummond, and V. I. Fal'ko, Phys Rev B 89, 205416 (2014)
[2] Zólyomi, V., N. D. Drummond, and V. I. Fal'ko, Phys Rev B 87, 195403 (2013)

Day 2

Session 2

Thursday, 8th December

11:15-13:00

Nanostructures
&
Poster Pitches

Modeling Energy Transfer Processes in GaN Quantum Wires

L. A. Th. Greif [1], S. Kalinowski[1], G. Callsen[1], J. Müßener[2], A. Schliwa[1], M. Eickhoff[2] and A. Hoffmann[1]
[1] Institut für Festkörperphysik, TU Berlin, Germany
[2] I. Physikalisches Institut, Justus Liebig-Universität Gießen, Germany

Spectrally sharp emission lines associated with self-assembled GaN/AlN quantum wires (QWRs) are pointing to low dimensional structures of high structural and optical quality [fig. 1]. The origin of the sharp luminescence lines is not established *a-priori* as there are at least three possible sources: the GaN-core, the GaN-disc or the GaN-wires, which are formed at the edges of the structure.

Time-resolved photoluminescence spectra reveal a quite complex excitation and decay pattern suggesting energy transfer and saturation processes to occur. The assignment of the different spectral features to the corresponding emitter regions is not possible without extensive electronic structure modeling. Doing this, one faces a more than ten-million atom problem requiring a hierarchical multi-scale approach to account for (i) strong and weak confinement regions, (ii) pyroelectricity, strain and the associated piezoelectric fields, (iii) Coulomb-based saturation effects and the ensuing shift of the photoluminescence. This is done by a combination of eight-band-kp theory, thus taking into account pyroelectricity, strain and pyroelectricity, the configuration interaction (CI) scheme for the strong-confinement region and the Hartree-Fock (HF) method to consider Coulomb interaction among carriers.

Thereby, we calculate transition energies and radiative lifetimes as functions of the carrier concentration as well as the exciton binding energy in the wire region. We expose significant parts of the carrier dynamics leading to an intense and deterministically tunable QW emission, summarizing the particular optical properties of GaN/AlN QWRs focusing energy transfer processes between all optically active regions. Such processes are the fundamental pre-requisite for any future electrical operation of such structures.

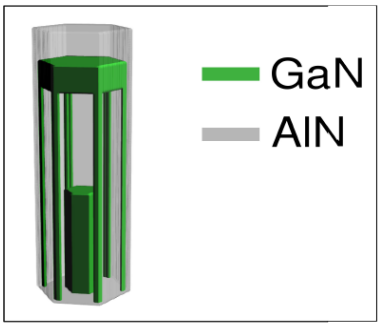

Figure 1: Schematic structure of an AlN/GaN nanowire heterostructure with embedded GaN quantum wires.

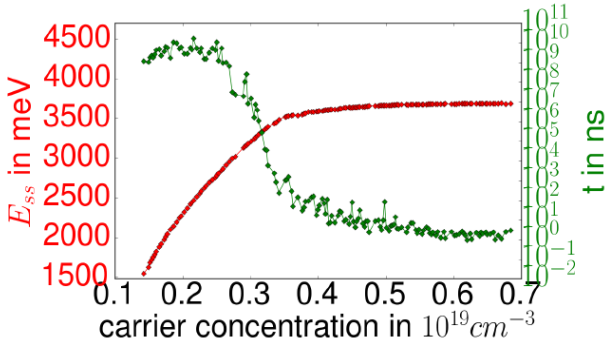

Figure 2: Simulation of the radiative lifetime (green) and the transition energy (red) as function of the carrier concentration.

Influence of strain relaxation in axial $In_xGa_{1-x}N$/GaN nanowire heterostructures on their electronic properties

Oliver Marquardt, Thilo Krause, Vladimir Kaganer, Michael Hanke, and Oliver Brandt
Paul-Drude-Institut für Festkörperelektronik, Berlin, Germany

The ternary alloy $In_xGa_{1-x}N$ constitutes the material of choice for the development of red-green-blue light emitting diodes (LEDs) for display technology, since its emission wavelength can in principle be tuned from the near-infrared to the ultraviolet via the In content x. However, the use of planar $In_xGa_{1-x}N$/GaN heterostructures for orange and red emission is problematic due to a large lattice mismatch between InN and GaN as well as due to the Stark effect resulting from large built-in potentials. These shortcomings can potentially be avoided by growing axial nanowire heterostructures: the free side facets facilitate elastic relaxation, which allows to maintain a high crystal quality even at large In contents and is expected to reduce or even completely eliminate the built-in potentials.

We have performed a systematic study of the impact of elastic strain relaxation on the built-in polarization potentials and the electronic properties of axial $In_xGa_{1-x}N$/GaN nanowire heterostructures. Strain and polarization potentials were computed using both analytical[1] (A) and numerical (H) approaches based on continuum elasticity and the Poisson equation. These quantities serve as input for an eight band **k·p** model to compute the wave functions and energies of the electron and hole ground states.

Our analysis reveals that strain relaxation reduces the polarization potentials, which in turn limits the range of accessible transition energies. For larger thicknesses, the transition energies thus approach a constant value, a behavior commonly associated with field-free systems (Fig. 1). Moreover, strain and polarization potentials induce complex, three-dimensional potential landscapes that induce confinement of electrons and holes in the center, at the edges or at the side facets of the $In_xGa_{1-x}N$ insertion, depending on its thickness and In content (Fig. 2).

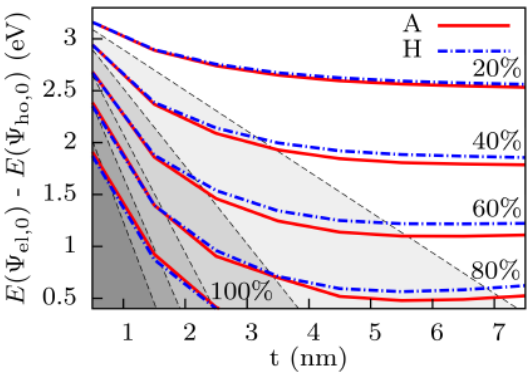

Fig. 1: Transition energies for different In contents as a function of the insertion thickness. Shaded gray areas depict transition energies of respective planar systems (x=20-100%: light to dark gray).

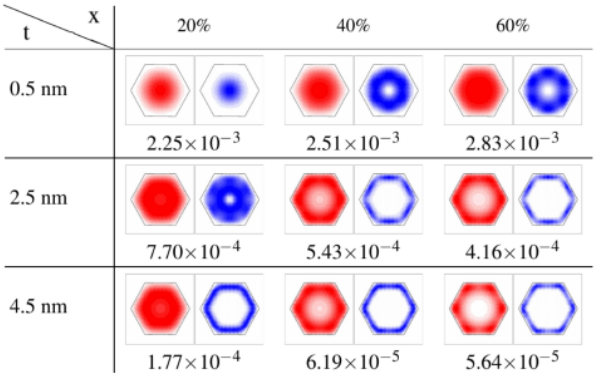

Fig. 2: Electron (red) and hole (blue) ground state charge densities in top view together with the respective electron-hole overlap (arbitrary units).

[1]V. M. Kaganer, O. Marquardt, and O. Brandt, Nanotechnology **27**, 165201 (2016)

Impact of random alloy fluctuations on the electronic and optical properties of site-controlled (111)-oriented InGaAs/GaAs quantum dots

R. Benchamekh[1] , S. Schulz[1] and E. P. O'Reilly[1,2]
[1]Tyndall National Institute, Cork, Ireland
[2]Department of Physics, University College Cork, Cork, Ireland

One of the main challenges to achieve quantum information applications is the design of efficient entangled photon generators. It has been proposed that semiconductor quantum dots (QDs) could produce a pair of polarisation entangled photons via a biexciton-exciton cascade[1]. However, QDs grown along the standard (001) direction are not ideally suited to entangled photon generation due to their C_{2v} symmetry. In contrast, site-controlled QDs grown on a (111) oriented substrate have been shown to emit entangled photons[2]. This is explained by a higher symmetry level (C_{3v}) which allows orthogonally polarised exciton states to be degenerate. In a real InGaAs QD, the random distribution of In and Ga cations inside the dot should break the C_{3v} symmetry and may therefore reduce the efficiency of actual systems.

Here, we use an $sp^3d^5s^*$ tight-binding model, including strain, first- and second-order piezoelectric effects, to investigate the electronic and optical properties of realistic site-controlled (111)-oriented InGaAs/GaAs QDs on an atomistic level. Using a pure InAs/GaAs QD as a reference system, we show that the combination of spin-orbit coupling and biaxial strain effects can lead to sizable spin-splitting effects in these systems. Then, a realistic InGaAs/GaAs QD with 25% InAs content is studied. Our analysis reveals that the impact of random alloy fluctuations on the electronic and optical properties of (111)-oriented InGaAs/GaAs QDs reduces strongly as the lateral size of the dot increases and approaches realistic sizes. For instance the optical matrix element shows an almost vanishing anisotropy in the (111)-growth plane (cf Fig. 1). Furthermore, conduction and valence band mixing effects in the system under consideration are strongly reduced compared to standard (001)-oriented InGaAs/GaAs systems. All these factors indicate a reduced fine-structure splitting in site-controlled (111)-oriented InGaAs/GaAs QDs. Thus, we conclude that dots with realistic (50–80 nm) base length represent promising candidates for polarization entangled photon generation, consistent with recent experimental data.

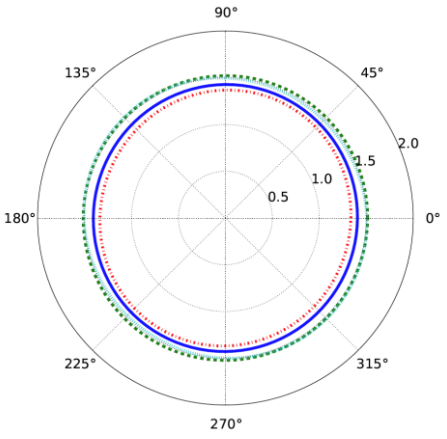

Figure 1: Angular dependence of the in-plane optical matrix element (in eV) of a $In_{0.25}Ga_{0.75}As$/GaAs QD with a triangular shaped base calculated within virtual crystal approximation (solid blue line) and three different alloyed configurations (Config.1: dashed green line, Config.2: dashed-dotted red line, Config.3: blue dotted line). The base length of the dot is 55 nm.

[1] O. Benson *et al*, *Phys. Rev. Lett*. 84, 2513 (2000)
[2] G. Juska *et al*, *Nature photonics*, 7, 527 (2013)

Elastic properties of semiconductors beyond the limit of infinitesimal strain

Daniel S. P. Tanner[1,2], Miguel A. Caro[3,4], Stefan Schulz[1,2], and Eoin P. O' Reilly[1,2]
[1]Tyndall National Institute, Cork, Ireland
[2]Department of Physics, University College Cork, Ireland
[3]COMP, Department of Applied Physics, Aalto University, Finland
[4]Department of Electrical Engineering and Automation, Aalto University, Finland

Valence force field (VFF) models are widely used to study the elastic properties of semiconductor alloys and heterostructures. However, given that standard VFF models include only terms up to second order in the atomic displacements, these will likely fail to describe aspects of systems with large strains. Figure 1 shows the calculated pressure on a zinc-blende AlN supercell under hydrostatic strain as determined by density functional theory (DFT), and the popular VFF models of Keating[1] and Martin[2]. This comparison clearly shows the shortcomings of VFF models for strains >~5%, which is a realistic local strain value around an Al or In atom in AlInN.

In order to improve the empirical description of the force fields, anharmonic corrections can be added to the interatomic potentials of the VFF models, allowing then for a fit to higher order elastic constants and internal strain parameters. In a first step, to develop an improved VFF model for a variety of III-V zinc-blende materials, we have performed hybrid functional DFT calculations to determine third order elastic constants. To properly describe the elastic properties of systems with large strains, the approximations of harmonic elasticity theory are no longer valid[3], and finite strain theory[4] must be used. In going beyond harmonic theory, new and more complex forms for the strain, stress, and the relation between them arise. Using these new stress-strain relations, the third order elastic constants can be extracted from the hybrid functional DFT calculations for different strain branches. Subsequently, fitting the force constants of a here developed modified VFF model to lattice constants and second- and third-order elastic constants will allow for an improved description of the elastic properties of heterostructures over a wider range of strains.

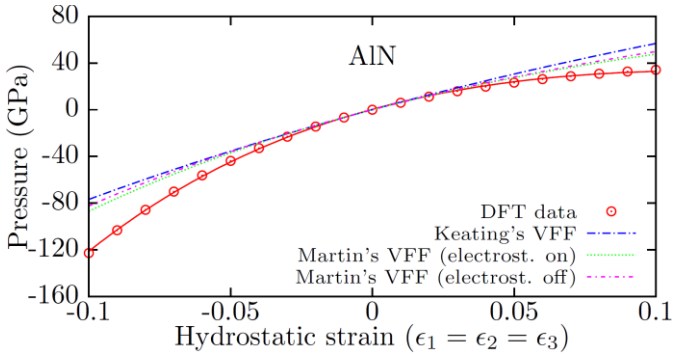

Figure 1: Pressure on a zinc-blende AlN supercell as a function of hydrostatic strain. Calculations have been carried out by means of DFT and the VFF models of Keating and Martin.

[1] P. N. Keating, Phys. Rev., 145, 637 (1966)
[2] R. M. Martin, Phys. Rev. B, 1, 4005 (1970)
[3] M. Lopuszynski et. al., Phys. Rev. B, 76, 045202 (2007)
[4] F. D. Murnaghan, Am. J. Math., 49, 235 (1937)

Theoretical model of threading dislocations strain and contrast in the scanning electron microscope images

Elena Pascal, Ben Hourahine and Carol Trager-Cowan
University of Strathclyde, Department of Physics, SUPA, Glasgow, G4 0NG, UK

The scanning electron microscope (SEM) proved itself a powerful nano-characterisation technique when applied to the semiconductors used in optoelectronic devices. The images produced contain sample modulated electron diffraction information. With a suitable model these images can offer a picture of the strain in the sample. Dislocations are such a source of strain and can be imaged in the SEM as long as they live close the surface.

High densities of dislocations are generally correlated to poor optoelectronic properties in GaN based devices. For threading dislocations (TDs) which propagate throughout the sample there is strong evidence to suggest that they behave as non-radiative recombination centres reducing the luminescent output and device efficiency.

In order to model the contrast observed in the SEM images linked with such TDs we employ Howie-Whelan[1] type equations to describe the diffraction of the electrons in the sample. The strain associated with the dislocation type is derived from continuum elasticity as formulated by Yoffe[2]. During diffraction the electrons have a finite probability of losing coherence and can scatter in a different direction. If that direction is towards the detector then it can contribute to the image collected. The scattering back of the electrons is described by the scattering matrix following the approach of Rossouw et al.[3]. We use Monte Carlo methods in order to derive the interaction volume of the electrons.

In this work we explore the model described above as applied for normal incidence threading dislocations in GaN type material and compare the resulting SEM dislocation contrast to experimental work. This work aims to provide TD identification techniques for the scanning electron microsope.

References

[1] Head A. K., Computed electron micrographs and defect identification. Vol. 7. Elsevier, 2012.
[2] E. H. Yoffe., Phil. Mag., 1961, 6, 1147.
[3] C. J. Rossouw, et al., Phil. Mag. A, 1994, 70, 985.

Band Alignment between Intermediate Band Material and $CuAlSe_2$ and ZnS

J.E. Castellanos Águila[1,2], P. Palacios[2,3], J. J. Arriaga[1], P. Wahnón[2]
[1]Instituto de Física, Benemérita Universidad Autónoma de Puebla, Av. San Claudio y 18 sur. C. U. 72000. Puebla, México
[2]Instituto de Energía Solar, ETSI Telecomunicaciones, Universidad Politécnica de Madrid, 28040 Madrid, Spain
[3]Dpt FAIAN, ETSI Aeronáutica y del Espacio, Universidad Politécnica de Madrid, 28040, Madrid, Spain

The study of interfaces between two materials, being one of them the intermediate band material $CuGaS_2$:Cr, and the processes that occurs in the interfaces are necessary for a better understanding of how these proposed materials operate in the entire structure of the solar cell. A proper description of the structure and electronic properties of surfaces and heterointerfaces must be taken into account in designing, fabricating and analyzing such heterostructures devices. In this work, we present a systematic procedure for the calculation of the energy band alignment at an abrupt IB material-semiconductor heterojunction. The accuracy of the method is believed to reflect directly the quality of the band structures. The alignment using as reference the average electrostatic potential predicts that the $CuGaS_2$:Cr/$CuAlSe_2$ and the $CuGaS_2$:Cr/ZnSe interface are type II and possess a staggered alignment. These are the appropriate conditions to match two interfaces into a heterostructure with three semiconductors ($CuAlSe_2$/$CuGaS_2$:Cr/ZnSe) so that electrons and holes photo-generated in the $CuGaS_2$:Cr absorber layer can be extracted selectively, as desired, at both device sides.

First principles modelling of tunnel field-effect transistors based on heterojunctions of strained Germanium/InGaAs alloy

Joao Abreu, Gabriel Greene and Myrta Gruning
School of Mathematics and Physics, Queen's University Belfast, United Kingdom

In the past decades technological advancements in electronic devices have occurred through the size reduction of field effect transistors (FETs)[1,2], their fundamental building blocks.

Nowadays the size reduction of FET has reached its physical limits and new solutions have to be considered[3]. In this project first principle modelling guides and assists experimental work on and engineering of tunnel field-effect transistors (TFETs)[4,5,6] based on heterojunctions of strained Germanium/InGaAs alloys compatible with the silicon technology. As an advantage over current metal-oxide-semiconductor FET, TFETs have a better on/off current ratio when performance requirements are moderate and can thus be used for low-power applications[7] (e.g. smartphones, GPS).

First principles calculations based on density functional[8] and many-body perturbation theory (MBPT)[9] approaches will explore how the chemical composition of the alloy and interface stoichiometry (Fig 1) that affects the electronic properties of the device, in particular the band offset at the interface[10] (Fig 2), and the strained germanium indirect-to-direct band transition.

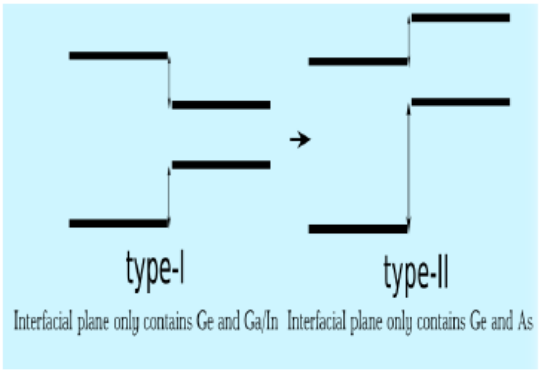

Fig 1. Heterojunction change from type-I to type-II

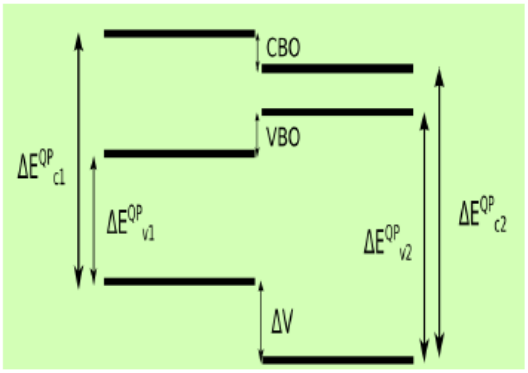

Fig 2. Bands offset in MBPT

References:
[1]C. C. Hu, "Modern Semiconductor Devices for Integrated Circuits", Pearson, 2009
[2]S. M. Sze and K. K. Ng, "Physics of Semiconductor Devices", Wiley-Interscience, 2007
[3]W. Arden and et al., "Towards a 'more-than-moore' roadmap", Report, CATRENE Scientific Committee, 2011
[4]S. H. Kim, H. Kam, C. Hu, and T. Liu, Germanium-source tunnel field effect transistor with record high ion/ioff, VLSI Tecnology, 2009
[5]M. Lee and et. al., Silicon nanowire-based tunneling field-effect transistors on flexible plastic substrates, Nanotechnology, 20, 2009
[6]S. Mookerjea and et. al., Experimental demonstration of 100nm channel length in0.53ga0.47as-based vertical inter-band tunnel field effect transistor (tfets) for ultra-low-power logic and sram applications, IEDM, 2009
[7]A. M. Ionescu and H.Riel, Tunnel field-effect transistors as energy-effecient electronic switches, Nature, 479, 2011
[8] P. Giannozzi and et. al. Quantum espresso: a modular and open-source software project for quantum simulations of materials, J. Phys: Condens. Matter, 21, 2009
[9] A. Marini et al. Yambo: an ab initio tool for excited state calculations, Comp. Phys. Comm. 180, 2009
[10] M. Giantomassi and et. al., Electronic properties of interfaces and defects from many-body perturbation theory: Recent developments and applications, Phys. Status Solidi B, 248, 2011

Multivariate numerical optimization of an InGaN-based hetero junction solar cell

Abdoulwahab Adaine[a,b], Sidi Ould Saad Hamady[a,b] and Nicolas Fressengeas [a,b]
[a] Université de Lorraine, Laboratoire Matériaux Optiques, Photonique et Systèmes, Metz, F-57070, France
[b] Laboratoire Matériaux Optiques, Photonique et Systèmes, CentraleSupélec, Université Paris-Saclay, Metz, F-57070, France

Nitride-based semiconductor materials are promising candidates for the manufacturing of very high efficiency solar cells. The Indium Gallium Nitride (InGaN) ternary alloy has a particular interest, because its energy gap can be varied in a wide spectral range just by changing the indium composition[1]. This can lead to bandgap engineering, which would to ease the design of multi-junction solar cells. Within this context, we simulated and optimized an InGaN-based dual-junction solar cell connected by a specifically designed tunnel junction. This allows the conversion of different parts of the solar spectrum, thus enhancing the solar light absorption efficiency and the photocarriers transport.

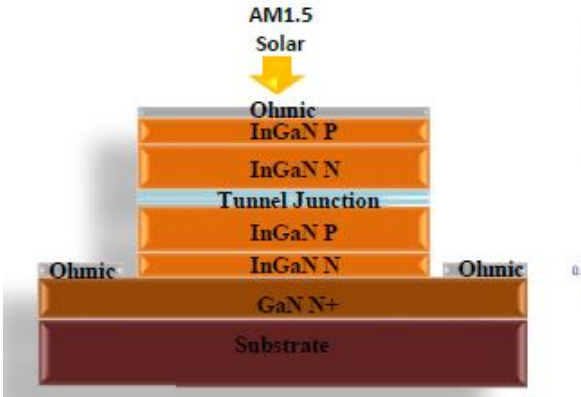

Figure 1: Schematic view of the solar cell structure under an AM1.5 spectrum

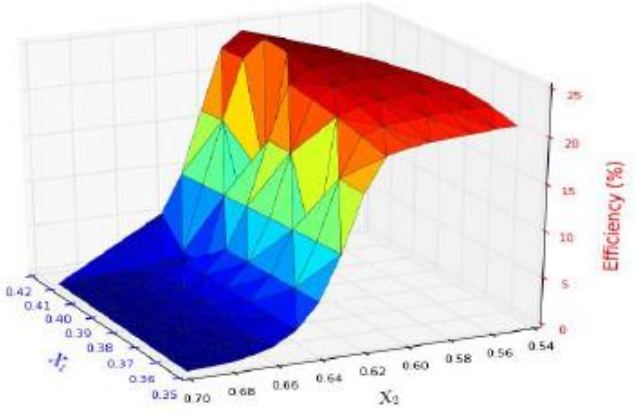

Figure 2: Efficiency as a function of the Indium compositions, X_1 for the top cell and X_2 for the bottom cell

The device is simulated in the framework of a drift-diffusion model using the ATLAS device simulation framework from the Silvaco company. The optimization is done by coupling ATLAS with multivariate mathematical optimization methods based on state-of-the-art optimization algorithms. For that, we used a Python package that we developed in the SAGE software interface.

The objective is to optimize the conversion efficiency of the solar cell by simultaneously optimizing several physical and geometrical parameters of the solar cell. It is an unprecedented multivariate optimization for solar cells which takes into account the correlation between these parameters.
For this solar cell, we optimized simultaneously 11 geometric and physical parameters of the structure. An optimum conversion efficiency of 24% was predicted for this designed solar cell. A detailed study of the impact of the tunnel junction and the various possible material defects on the efficiency has been conducted. This includes the influence of the piezoelectric field distribution and hetero-interface traps. These results are compared to previously proposed Schottky based design.[2] [3]

[1] C. A. M. Fabien, W. A. Doolittle, Guidelines and limitations for the design of high-efficiency InGaN single-junction solar cells, Solar EnergyMaterials and Solar Cells 130 (2014)
[2] Sidi Ould Saad Hamady, Abdoulwahab Adaine, and Nicolas Fressengeas. "Numerical simulation of InGaN Schottky solar cell." Materials Science in Semiconductor Processing 41 (2016)
[3] Abdoulwahab Adaine, Sidi Ould Saad Hamady, and Nicolas Fressengeas. "Simulation study of a new InGaN p-layer free Schottky based solar cell." Superlattices and Microstructures 96 (2016)

Effect of thermal annealing on the performance of type-II GaSb/GaAs quantum dots solar cell

Hela Boustanji, Sihem Jaziri and Stanko Tomic
Laboratoire de Physique de la Matière Condensée, Faculté des Sciences de Tunis, 2092 El Manar, Tunisie
Laboratoire de Physique des Matériaux, Faculté des Sciences de Bizerte,7021 Jarzouna, Tunisie
Joule Physics Laboratory, School of Computing, Science and Engineering, University of Salford, Manchester M5 4WT, United Kingdom

This work represents a theoretical analysis of the effect of thermal annealing on the performance of type II GaSb/GaAs quantum dots solar cell (QDs SC). Due to interdiffusion process, our theoretical results show a significant enhancement in the absorption spectrum and holes escape mechanism. Therefore, we discuss how the overlap between electron and hole are strongly varied after thermal treatment [1]. The obtained results show the low annealed temperature 733K lead to enhance the infrared absorption which is due to the spatial separation of carriers. This behavior is explained by the redshift in the intraband optical absorption spectrum. However after high-temperature annealing 900-1200K, the probability that electron-hole pairs recombine increases when the confined QD energy states shift to the WL. Consequently, the QD is modified to a quantum well like structure which is caused by the total dissolution of the QD in the WL [2]. Holes that are photogenerated start to populate the WL. Therefore, the radiative recombination rate is expected to be enhanced similar to type-I systems [3]. We assign this enhancement to an increase in the oscillator strength. For this, we note the blue shift of the interband absorption spectrum. Holes that are accumulated should escape out the dot before they can recombine and will contribute to enhance the photo response of QDSC. Holes escape process was calculated and found to be 10^{-12}- 10^{-14}s which is much faster than the radiative recombination$10^{-7} - 10^{-9}$s .This behavior promises the improvement of the photocurrent of the QDSC.

1 T. Kawazu, T. Noda, T. Mano, Y.Sakuma, and H.Sakaki, J. Appl. Phys. 51, 115201(2012)

[2] T. Kawazu, T.Noda, T. Mano, Y. Sakuma and H.Sakaki, J. Appl. Phys.54, 04DH01 (2015)

[3] Wei-Ting Hsu, et al., Physica E: Low-dimensional Systems and Nanostructures 42, 2524 (2010)

AlGaInP-based Quantum Dot LEDs as efficient red light sources

Silviu Bogusevschi[1,3], Andrea Pescaglini[2], Emanuele Pelucchi[2,3] and Eoin P. O'Reilly[1,3]
[1]Photonics Theory Group, Tyndall National Institute, Cork, Ireland
[2]Epitaxy and Physics of Nanostructures Group, Tyndall National Institute, Cork, Ireland
[3]Department of Physics, University College Cork, Cork, Ireland

Commercially available red Light Emitting Diodes (LEDs) typically operate in the 630 – 650 nm spectral range, where the human eye has a relatively low spectral response. Shifting the emission wavelength towards 610 nm would strongly improve the eye response, thereby reducing the output required from the LED devices. However, the critical issue faced by shorter wavelength devices is the decrease in the quantum efficiency because of the reduced carrier confinement and increased carrier leakage with decreasing wavelength. This presents a major challenge for the development of efficient LED sources for future handheld devices and wider applications and has been addressed e.g. by using numerous AlGaInP Quantum Wells (QW) in the active region[1] or InGaN as an emitting material with its wide range of bandgaps[2].

We address here the potential benefits of using AlGaInP-based Quantum Dot (QD) structures to improve the radiative recombination efficiency and device characteristics of shorter wavelength red LEDs. We use the 8-band **k·p** model implemented within the semi-analytical planewave expansion method to investigate how the QD direct-gap ground state emission energy depends on the dot size, shape and composition, as well as on the assumed barrier layer composition. The calculations treat the effects of strain on the electron and hole states, as well as the overlap between the electron and hole wavefunctions. We separately use the one-band effective mass model to investigate the effect of the built-in strain on the X-related states in the dot and surrounding material. We benchmark the theoretical model by comparing our results with experimental measurements on a series of stacked QD structures grown on GaAs, which helps us having a better understanding of the physical processes in such structures. Finally, using the obtained data we provide guidelines for device optimisation in order to improve their overall efficiency.

[1]Shim, Jong-In et al., *Efficiency droop in AlGaInP and GaInN light-emitting diodes*, Applied Physics Letters, **100**, 111106 (2012)
[2]S. Jahangir et al., *Red-Emitting (λ= 610 nm) $In_{0.51}Ga_{0.49}N$/GaN Disk-in-Nanowire Light Emitting Diodes on Silicon*, Journal of Quantum Electronics, **50**, 7 (2014)

Theoretical study of the optical properties of a-plane InGaN/GaN quantum dots

Saroj Kanta Patra[1,2], **Stefan Schulz**[1]
[1]**Tyndall National Institute, University College Cork, Cork**
[2]**Department of Electrical Engineering, University College Cork, Cork**

InGaN/GaN quantum dots (QDs) are of great topical interest due to their potential for single-photon sources emitting in the visible part of the spectrum [1]. Thanks to their large band offsets and higher exciton binding energies, single-photon emission near room temperature can in principle be achieved [2]. However, usually nitride-based dots are grown on polar planes, suffering from a strong quantum confined Stark effect (QCSE), thereby reducing their recombination efficiency. Alternatively, dots grown along a nonpolar direction are advantageous since they exhibit reduced built-in fields and increased oscillator strength. In this work, we present a detailed study of the electronic and optical properties of nonpolar InGaN/GaN QDs by means of a plane-wave based multiband **k.p** model. Coulomb effects are accounted for by coupling the **k.p** model with self-consistent Hartree calculations. The impact of the QD size and geometry on built-in potential, excitonic and biexcitonic properties is studied and the results are compared with corresponding c-plane systems. Our calculations reveal that inspite of exhibiting strongly reduced built-in fields when compared to polar dots, exciton and biexciton properties are significantly affected by these residual fields. For instance, the changes in these fields, arising from the changes in the QD geometry result in an unusual variation of an initial decrease and then increase in the exciton binding energies E_x^b as shown in Fig. 1 [3]. Moreover, we find that the attractive Coulomb interaction between electrons and holes overcomes the spatial separation of the carrier wavefunctions due to the presence of the built-in field, resulting in a fast-recombination lifetime τ. Furthermore, τ has been calculated for varying QD sizes and is found to be in good agreement with experimental results. Additionally, our results indicate that nonpolar dots produce a very high degree of optical linear polarization (DOLP), which is almost insensitive to shape anisotropies and In content changes (cf. Fig. 2) [4]. All of the above results indicate that nonpolar InGaN/GaN QDs are potential candidates for next generation polarized single-photon sources.

[1] S. Deshpande et al., **Nat. Commun**. 4,1675--8 (2013)
[2] M . J. Holmes et al., **ACS Photonics** 3, 543-546 (2016)
[3] S. K. Patra, S. Schulz (submitted) (2016)
[4] Tong Wang et al. (submitted) (2016)

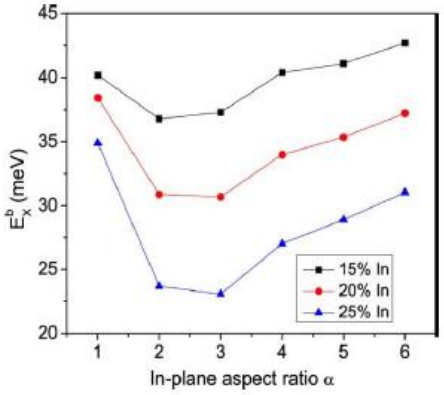

Fig 1: Exciton binding energy E_x^b as a function of in-plane aspect ratio α for different indium concentrations.

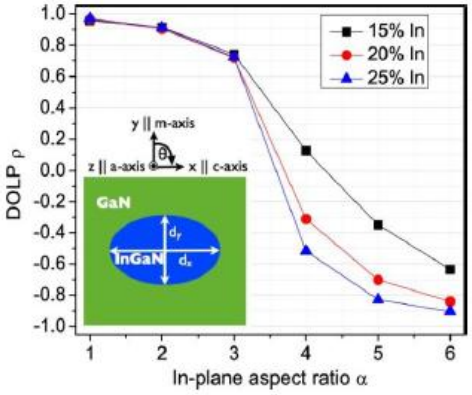

Fig 2: DOLP ρ as a function of the in-plane aspect ratio α and In content for lens-shaped a-plane InGaN/GaN QD.

Electronic properties of GaAs crystal phase nanostructures

Oliver Marquardt, Pierre Corfdir, Manfred Ramsteiner, Lutz Geelhaar, and Oliver Brandt
Paul-Drude-Institut für Festkörperelektronik, Berlin, Germany

GaAs has two polytypes crystallizing in the equilibrium zincblende (ZB) and the wurtzite (WZ) structure, that are frequently observed to coexist as stacked sequences along the axis of GaAs nanowires. As the two polytypes exhibit different band gaps, one can perform band gap engineering by designing *crystal-phase nanostructures*. These nanostructures have several advantages in comparison to conventional heterostructures: Polytype segments are essentially free of strain, do not suffer from alloy disorder, and exhibit atomically flat interfaces. Recently, much progress has been achieved in controlling the occurence of polytypism in GaAs NWs.

Previous theoretical models of the electronic properties of GaAs crystal-phase nanostructures have neglected an important detail of the band structure, namely the existence of the two energetically close conduction bands (CBs) with Γ_7 and Γ_8 character at the center of the Brillouin zone of the WZ. While the Γ_7 CB is equivalent to the Γ_6 CB of the ZB phase, the Γ_8 CB has no such equivalent. Therefore, a ZB segment acts as a large barrier for an electron confined in the Γ_8 CB. Moreover, this band has a very large effective mass along the NW axis, giving rise to strong confinement.

We introduce a ten band **k·p** model in order to allow an explicit treatment of both relevant conduction bands. As the energy ordering of the two CBs is still under debate, we evaluate two different parameter sets. We then perform systematic studies of the electronic properties of purely WZ GaAs NWs and of superlattices consisting of ZB and WZ segments. We find that confinement, character, and energies of the energetically lowest electron states exhibit distinct features that can be described correctly only if both CBs are taken into account (Fig. 1). Our study reveals that intersecting, but not interacting potential landscapes formed from the $\Gamma_{6,7}$ and the Γ_8 CB provide a possible explanation for the wide range of emission energies reported for polytypic GaAs NWs.

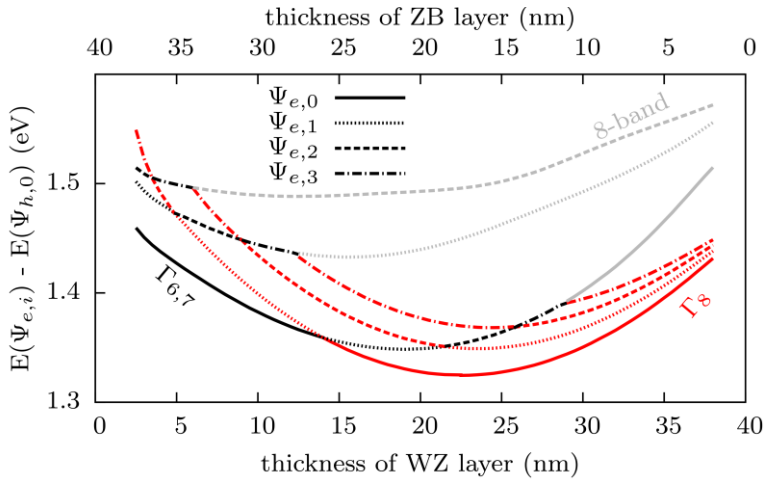

Fig. 1: Energy difference between the four energetically lowest electron states and the hole ground state as a function of the WZ segment thickness in a WZ/ZB superlattice of 40 nm period. Red lines indicate a Γ_8 character, black ones a $\Gamma_{6,7}$ character. Gray lines depict the respective behaviour as found when employing an eight band **k·p** model.

Configurational effects on the piezoelectricity of semiconductor alloys: the case of ScAlN

Miguel A. Caro
Department of Electrical Engineering and Automation, Aalto University, Espoo, Finland

Piezoelectricity arises in heteropolar tetrahedral semiconductors as a consequence of the point group of their crystal structures (zinc-blende and wurtzite). Piezoelectricity can be both the cause of degraded device performance, e.g. loss of recombination in nitride-based LEDs, or constitute the very working principle of some systems, for instance piezoelectric resonators used in micro electromechanical systems (MEMS). While some researchers are striving to reduce the piezoelectric response of these materials for light production, others are trying to enhance it for devices that rely on electromechanical coupling for their operation.

ScAlN has emerged as a promising substitute material for AlN in thin film piezoelectric devices, because of a several-fold increase in its piezoelectric coefficient. However, piezoelectric semiconductor alloys suffer from a strong dependence of the local piezoelectric response on the local alloy microstructure [1], such as random alloy fluctuations and localized lattice distortions. We will discuss the challenges present when trying to simulate this material using density functional theory in order to obtain an accurate and reliable description of its piezoelectric properties [2].

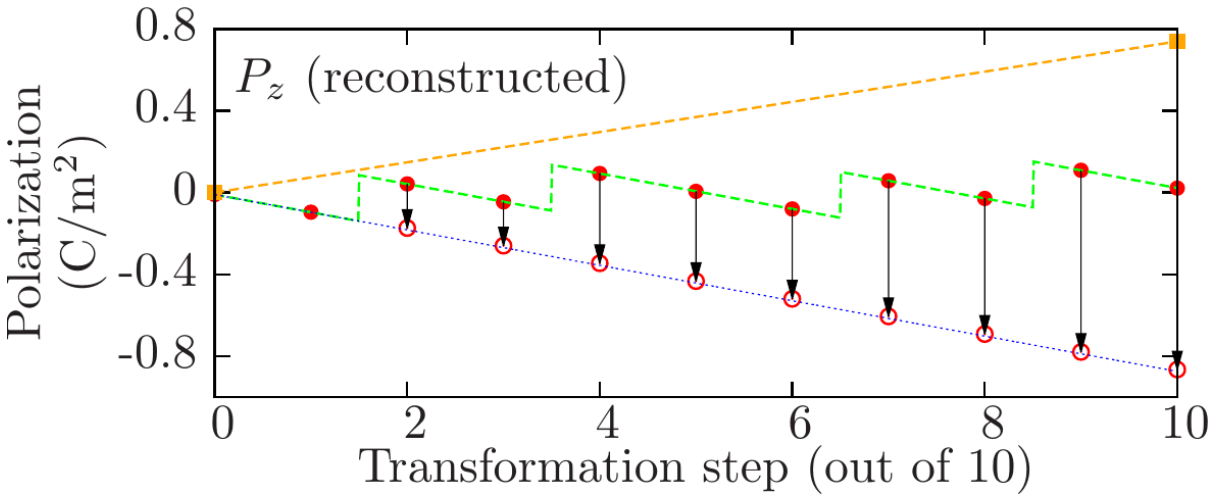

Illustration 1: Reconstruction needed to retrieve the spontaneous polarization of ScAlN [2]

[1] M.A. Caro, S. Schulz, E.P. O'Reilly, Physical Review B 88, 214103 (2013)
[2] M.A. Caro et al., Journal of Physics: Condensed Matter 27, 245901 (2015)

Direct band gaps from GeSn alloys: A hybrid functional density functional theory based analysis

Edmond O'Halloran[1,2], Stefan Schulz[1], Eoin O'Reilly[1,2],
[1]Tyndall National Institute, Lee Maltings, Cork, Ireland
[2]Department of Physics, University College Cork, Cork, Ireland

A fundamental issue with Si-Ge semiconductor alloys is the indirect nature of the fundamental band gap, which results in materials that are inefficient absorbers and emitters of light. The development of efficient light emitters based on group IV elements however demands a direct-gap semiconductor system. As a result semiconducting alloys of Si, Ge and Sn have been attracting a large amount of research attention as a means of producing direct band gap semiconductors that are compatible with conventional Si technology.[1] These semiconductors would have prospective applications in very efficient future optoelectronics.

To analyze the electronic structure of GeSn alloys we have performed DFT calculations based on Heyd-Scuseria-Ernzerhof (HSE) screened exchange hybrid functionals. In contrast to previous studies, supercells that allow for the mixing of Γ, L and X states have been constructed. Pressure dependent calculations indicate that for as little as 6% Sn in Ge, a significant mixing between Γ, L and X states occurs. To shed more light on the electronic structure of GeSn alloys, band unfolding techniques[2] have been applied, confirming the mixing between the different states. An example of an unfolded band structure for GeSn from a 16-atom fcc supercell is shown in Fig.1. Overall, our results reveal that, once band-mixing effects are accounted for, there is not a sharp transition of indirect to direct band gap in GeSn alloys.

Given the fact that HSE-DFT is computationally extremely demanding and thus limiting the analysis to small supercells, approaches such as the modified-Becke-Johnson LDA (mBJ-LDA) potential[3] are used here to extend our analysis to larger supercells. In doing so, it allows us to study in detail the band gap evolution of GeSn alloys with varying Sn concentrations over a wider range, shedding therefore light on the fundamental properties of GeSn alloys.

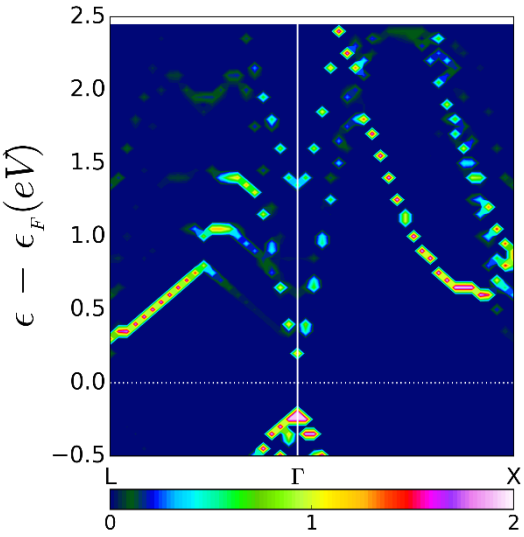

Figure 2: Effective band structure of $Ge_{15}Sn_1$ fcc supercell. The colour scale represents a weight to each point depending on the number of primitive cell bands crossing in each point.

[1]C. Eckhardt, K. Hummer and G. Kresse, Phys. Rev. Lett 89,165201 (2014).
[2]P. V. C. Medeiros, S. Stafström, and J. Björk, Phys. Rev.B 89, 041407(R) (2014).
[3]F. Tran and P. Blaha, Phys. Rev. Lett. 102, 226401 (2009).

Tunnel Injection Transistor Lasers: A Group IV Material based Analysis

Neetesh Kumar and Rikmantra Basu
Electronics and Communication Engineering Department National Institute of Technology Delhi Narela 110040, New Delhi, India

Transistor Lasers (TLs) have the potential for much faster broadband communication for long-haul networks as well as short haul connections for inter-chip and intra- chip communication for photonic integrated circuits [1]. Experimental and theoretical studies on TLs have considered so far single Quantum Well (SQW) and multiple Quantum Wells (MQWs) incorporated in the base of a Heterojunction Bipolar Transistor (HBT) [1, 2]. Work on IIIrd group material has been done in past but IIIrd group material has the limitation of not having integration on the same chip which is the important attraction of IVth group material so in this work we have chosen GeSn as TL material. Threshold base current and modulation response are estimated for InGaAs and GeSn based multiple quantum well tunnel injection transistor laser structure. Since IV group material has the advantage of integration so we have chosen GeSn as the material. GeSn device show higher threshold current and lower modulation bandwidth but the results are comparable.

Some of the results are as follows

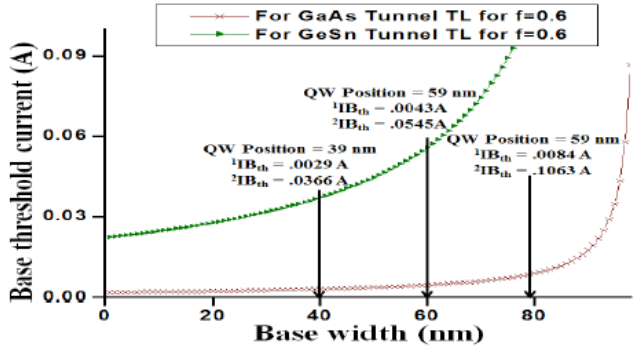

Fig 1(a): Base threshold current along the base of InGaAs TL and GeSn TL

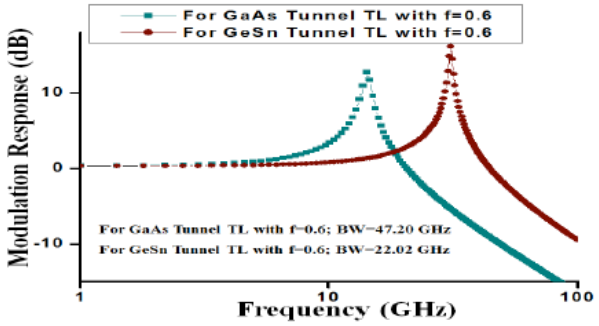

"Fig 1(b): Small signal modulation response for GeSn TL and InGaAs TL

Figure 1(a) displays the variation of base threshold current for the two TLs. The values for GeSn TL are of the same magnitude, but higher. Figure 1(b) shows the modulation response for both TLs. The resonance frequency and consequently the modulation bandwidth (BW) are substantially higher for InGaAs in comparison to the GeSn TL.

References:

[1]. H. W. Then, M. Feng, and N. Holonyak Jr, "The Transistor Laser: Theory and Experiment" Proc. IEEE, 101, 10, 2271-2298, 2013.
[2]. P. K. Basu, B. Mukhopadhyay and Rikmantra Basu, Semiconductor Laser Theory, CRC Press, Boca Raton, 2015, chapter 15.
[3]. R Basu, B. Mukhopadhyay, and P. K. Basu, "Analytical model for the threshold base current of a transistor laser with multiple quantum wells in the base", *IET Optoelectron*., vol. 7(3) , pp. 1-6 , 2013.
[4]. Rikmantra Basu, BratatiMukhopadhyay and P K Basu "Estimated Threshold Base Current and Light Power Output of a TL with InGaAs QW in GaAs Base" *Semiconductor Sc. and Tech.*,vol. 26, pp. 105014 (1-6), 2011.
[5]. R. Basu, B. Mukhopadhyay and P. K. Basu,"Modeling resonance-free modulation response in transistor lasers with single and multiple quantum wells in the base", *IEEE Photonics J*., vol. 4(5), pp. 1572-1581, 2012.
[6]. See Chapter 14 of Ref. [2].
[7]. M. Kucharczyk, M. S. Wartak, P. Weetman, and P.-K. Lau," Theoretical modeling of multiple quantum well lasers with tunneling injection and tunneling transport between quantum wells", *J. Appl. Phys.,* vol. 86, pp. 3218-3228, 1999.
[8]. V. V. Lysak, H. Kawaguchi, and I. A. Sukhoivanov, "Gain spectra and saturation power of asymmetric multiple quantum well semiconductor, optical amplifiers" *IEE Proc. Optoelectron.,* vol. 152(2), pp. 131-139, 2005.

Engineering $SrTiO^3/LaAlO^3$ heterostructures thickness: an ab initio study

Federico Iori
Universite' Paris Sud - CNRS, ORSAY, France

The possibility to achieve conducting and superconducting properties at the interface between two bulk insulator oxides as $SrTiO_3$ (STO) and $LaAlO_3$ (LAO) in 2004 [1] has wide opened the route toward the discovery and control of broad functional emerging properties in different oxides heterostructures. Nonetheless the STO/LAO system still present not clarified questions concerning the possibility to control the presence of the 2DEG at the interface. In this work we present our theoretical results supported by experimental measurements concerning the possibility to tune the critical thickness of the LAO topmost layer through the deposition of a metallic capping layer at the surface. Our ab initio Density Functional Theory calculations show how different metallic contact can lead to a reduction of the LAO critical thickness of 4 u.c. still preserving the 2D electronic gas at the interface.

[1] Otomo and Hwang, Nature 427, 423 (2004)

Ceria-Titania Interfaces for CO_2 and Water Activation

Stephen Rhatigan and Michael Nolan
Tyndall National Institute, University College Cork, Ireland

The development and deployment of artificial photosynthesis will enable a sustainable approach to generating, storing and using energy for the benefit of society as a whole. However, there is still much work to be done, in particular finding materials that will activate water and CO_2 either using photoexcitation or solar thermochemical processes. Common to each approach is the interaction of the molecule of interest with a heterogeneous catalyst. Tuning the structure and composition of the catalyst provides a path towards activating water and CO_2 and here materials modelling is crucial as it allows for screening of candidate materials and gives deep insights into fundamental processes taking place during these reactions. In this poster we will present our work on CeO_2-TiO_2 interfaces using density functional theory (DFT) simulations, exploring (1) formation of CeO_2-TiO_2 interfaces and their effect on energy gaps and oxygen vacancy formation, which will inform us as to the formation of reduced Ce or Ti species and (2) the interaction of water and CO_2 at stoichiometric and reduced CeO_2-TiO_2 structures, assessing the ability of these composite systems to activate these molecules.

Study of the impact of electrodes in the electron transport through Guanine and 8-oxoGuanine

Luke Wilson and Antonio Martinez
College of Engineering, Swansea University, United Kingdom

The unique charge conducting properties of DNA have shown that in principle it can be used to detect disease by variations in current[1]. Oxidative stress consequently forms DNA lesions leading to cell death, Guanine (G) is the most susceptible to oxidation and 8-oxoGuanine (8- oxoG) has been shown to be a good biomarker of oxidative stress and elevated levels are a risk factor for cancer[2]. Although substantial work has been performed, the transport through large DNA molecules is still poorly understood. Alternatively, single DNA bases have a less complex structure and its transport can be related to the HOMO-LUMO gap. We have concentrated on a single G base due to its higher oxidation potential and the influence of electrode geometry can be easily elucidated; with the hope to shed light on the transport through large DNA chunks. Density functional theory (DFT)/ Non-Equilibrium Greens Functions (NEGF) simulations were carried out using TranSIESTA[3]. Two different geometries of an Au(111) electrode have been considered (flat and pyramid). As the distance between molecule and electrode is difficult to control experimentally, two different electrode distances have been simulated. Fig. 1 shows the LUMO of the oxidised molecule. Our calculated MO shapes and HOMO-LUMO gap concur with previous studies[4]. I-V characteristics for G and 8-oxoG in Fig.2 show a 2.6 times increase in current at 3V for the geometry depicted inset; this is decreased dramatically when the geometry is modified. As electrode-molecule separation is increases, current decreases. These results provide a possible framework for detecting DNA oxidation and degradation.

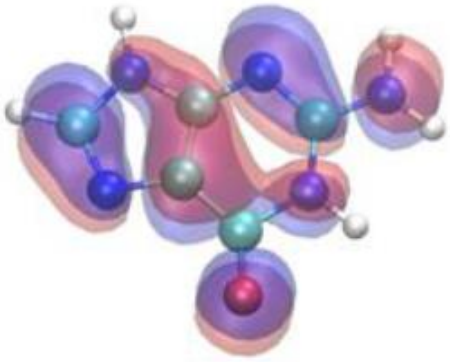

Figure 1 LUMO of 8-oxoG calculated using SIESTA[5].

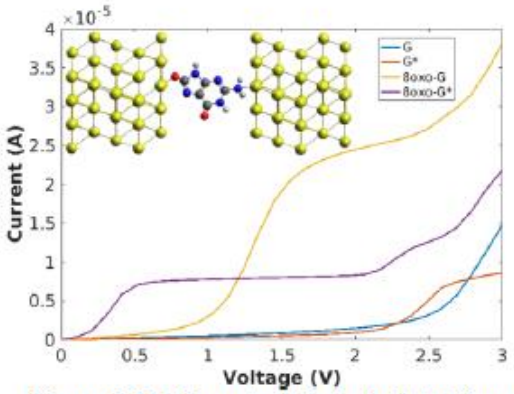

Figure 2 I-V characteristics calculated from transmission spectra, electrode molecule separation is 1.2 Å. *Modified Geometry.

1 M.P. Anantram and J.Q. Qi, Ieee International Electron Devices Meeting, 1006(1):212-26 (2013)
2 L.L Wu, C.C Chiou, P.Y. Chang, J.T. Wu, Clinica Chimica Acta, 339 (1-2), 1-9 (2004)
3 Stokbro K et al, Annals of the New York Academy of Sciences, 1006, 212-226 (2003)
4 S Kilina et al. Journal of Physical Chemistry C, 111(39):14541-51, (2007)
5 Soler JM et al, Journal of Physics-Condensed Matter, 14(11):2745-79 (2002)

Semi-empirical time-dependent DFT for plasmonic systems

Ben Hourahine
SUPA, Department of Physics, University of Strathclyde, John Anderson Building, 107 Rottenrow, Glasgow G4 0NG United Kingdom

Ground, and increasingly excited state, properties of nanosystems are now commonly calculated via linear-response density functional theory. There are a variety of formulations of this approach for DFT methods (coupled-perturbed equations, Casida equations, Sternheimer equations, ...), where the static or time dependent response of the system is calculated for chosen perturbations. In turn, the faster density- functional based tight binding method (DFTB[1]) has similarly successfully applied many of these approaches[2,3], with good accuracy and substantially lower computational costs than full DFT. In this contribution, the possibilities of using DFTB to rapidly evaluate plasmonic properties of large systems will be explored, discussing several of the approaches implemented within the framework of the DFTB+ code.

In particular, response calculations for graphene flakes and spin-orbit dominated metallic nano-particle systems containing ~1000 atoms on desktop class computers and larger structures on parallel computing platforms will be demonstrated.

[1] B. Aradi, B. Hourahine, and Th. Frauenheim, *J. Phys. Chem. A* **2007** *111*, 5678-5684 DOI: 10.1021/jp070186p
[2] T. A. Niehaus, S. Suhai, F. Della Sala, P. Lugli, M. Elstner, G. Seifert, and T. Frauenheim, Phys. Rev. B 63, 085108 (2001)
[3] T. A. Niehaus, D. Heringer, B. Torralva, and T. Frauenheim, Importance of electronic self-consistency in the TDDFT based treatment of nonadiabatic molecular dynamics, Eur. Phys. J. D 35, 467 (2005).

The local electron interaction with crystal lattice defects in cadmium telluride: ab initio approach

Orest Malyk
Semiconductor Electronics Department, Lviv Polytechnic National University, Ukraine

In the series of papers[1-4] the author presented a new approach for consideration of the transport phenomena on the base of the short-range principle to describe the process of the charge carrier scattering on the point lattice defects in II-VI and III-V compounds. However, the proposed approach has one major disadvantage – the presence of several fitting parameters which left some (albeit minimal) ambiguity in the choice of theoretical curves and also require the presence of experimental data to select the numerical values of fitting parameters. In the new approach the calculation of the charge carrier transition probabilities was carried out on the base of wave function determined from first principles using ABINIT code[5]. During this the exact integration over the volume of the zinc blende unit cell was used. When considering the electron scattering on acoustic and nonpolar optical phonons the acoustic and optical deformation potentials for the conduction electrons were calculated: E_{AC}=3.2 eV, E_{NPO}=12.96 eV. The calculation of the electron scattering on the ionized and neutral impurity, polar optical, piezoelectric (piezoacoustic and piezooptic) phonons was made without fitting parameters.

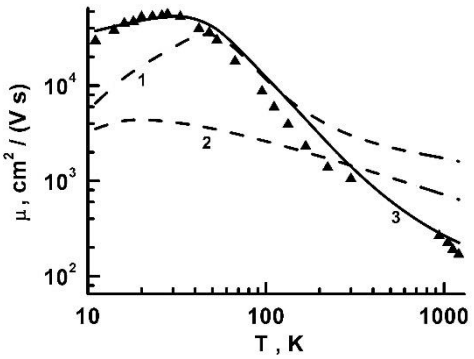

Fig.1. Electron mobility versus temperature in CdTe. 1,2 - long-range models (relaxation time approximation): 1- $\hbar\omega >> kT$, 2 - $\hbar\omega << kT$; 3-short-range models. Experiment – [6] .

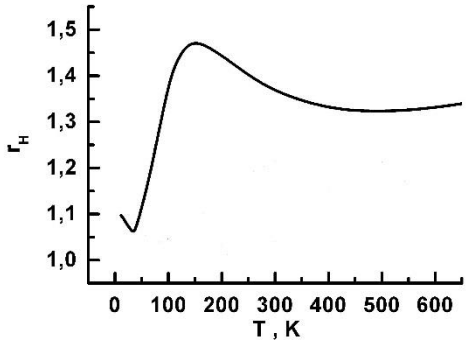

Fig.2. Temperature dependence of electron Hall factor

The temperature dependence of the electron mobility in the range 10 - 1200 K in cadmium telluride is calculated. It was established that the theoretical curve calculated on the basis of short-range models give a much better qualitative and quantitative agreement with experiment compared with the long-range scattering models (relaxation time approximation). The temperature dependence of the electron Hall factor is calculated.

[1] O.P. Malyk, Mater Sci Eng B 129**,** 161 (2006)
[2] O.P. Malyk, Phys Status Solidi C 6, S86 (2009)
[3] O.P. Malyk, Diamond Relat Mater 23, 23 (2012)
[4] O.P. Malyk, Can J Phys 92, 1372 (2014)
[5] X. Gonze et al , Comput Phys Commun 180, 2582 (2009)
[6] B. Segall et al Phys Rev 129, 2471 (1963)

Day 2

Session 3

Thursday, 8th December

14:45-16:00

DFT & Fundamentals

Charge transfer at organic-inorganic interfaces

Patrick Rinke
Department of Applied Physics, Aalto University, Helsinki, Finland

Future technologies will require new paradigms in design, functionality, scalability and a reduction in power consumption to meet our global energy challenges, reduce our environmental footprint and sustain or evolve the information age. Hybrid inorganic-organic systems (HIOS) offer a promising route because they may combine the best features of two distinct material classes or even achieve entirely new synergies.

In this presentation, I will present a quantum mechanical perspective of HIOS. I will first address molecular layers of strong acceptors that are used to change the work function of inorganic semiconductors. Focussing on the level alignment of ZnO-based HIOS interfaces, I will show that the build-up of space charge layers and the associated band-bending, that are common text book knowledge for inorganic semiconductors, can have profound and unexpected effects at the interface [1]. Then, I will address charge carrier dynamics. For ZnO we have recently identified hole polarons by combining infrared reflection-absorption spectroscopy with our quantum mechanical calculations [2]. The formation of these pseudoparticles might affect charge transport across HIOS interfaces. Last, I will address the question whether charge at organic-inorganic transfers to a molecule as a whole unit (integer charge transfer (ICT)) or resides on several molecules simultaneously (partial charge transfer (PCT)). For tetracyanoethene (TCNE) molecules adsorbed on an NaCl-passivated Cu(100)-surface we observe signatures of the charge-transfer mechanism in several observables, such as valence and core spectra and the bond length distribution of the individual molecules [3]. With our DFT formalism we can now discriminate between ICT and PCT.

[1] Y. Xu, O. T. Hofmann, R. Schlesinger, S. Winkler, J. Frisch, J. Niederhausen, A. Vollmer, S. Blumstengel, F. Henneberger, N. Koch, P. Rinke, and M. Scheffler, Phys. Rev. Lett. **111**, 226802 (2013)
[2] H. Sezen, H. Shang, F. Bebensee, C. Yang, M. Buchholz, A. Nefedov, S. Heissler, C. Carbogno, M. Scheffler, P. Rinke, and C. Wöll, Nat. Commun. **6**, 6901 (2015)
[3] O. T. Hofmann, P. Rinke, M. Scheffler and G. Heimel, ACS Nano **9**, 5391 (2015)

Mechanism for Oxygen Vacancy Accumulation Under Electron Injection Conditions in Amorphous Silicon Oxides

Manveer Singh Munde and David Gao and Alexander Shluger
Department of Physics and Astronomy, University College London, United Kingdom

Amorphous silicon oxides are a key component as insulting layers in CMOS devices and potential future application in ReRAM technology has been of recent interest. In both cases of hard[1] and soft[2,3,4] breakdown, the accumulation of oxygen vacancies is believed to result in a Si-rich conductive path. The exact mechanism for vacancy accumulation remains unresolved. In this work we use hybrid density functional theory calculations combined with the climbing-image nudged elastic band method to determine a mechanism for oxygen vacancy accumulation under electron injection conditions.

Our initial calculations on amorphous SiO_2 cells indicated that it is energetically favourable for oxygen vacancies to trap up to two electrons under typical device operating conditions. Total energies were used to estimate a mean value of ≈1.5 eV for the thermal ionisation energy of a trapped electron. We then studied the diffusion of oxygen vacancies to nearest neighbour sites in the charge states q=0,-1,-2 as a mechanism for vacancy accumulation. Mean activation energies on the order of 5 eV, 3 eV, and 2 eV indicated that electron trapping greatly facilitates vacancy diffusion. However, these values were larger than the corresponding ionisation energies in the majority of cases. Furthermore, our calculations on di- and tri-vacancy clusters revealed no energetic preference for vacancy accumulation by diffusion.

At some vacancy sites, double electron trapping was observed to facilitate the formation of an oxygen double bridge interstitial[3,5] and di-vacancy with an activation energy of ≈1 eV and under. Such interstitials can diffuse at a low energy cost of ≈0.2 eV[2,5]. Our calculations suggest that oxygen vacancies can accumulate through a correlated mechanism whereby electron trapping at vacancy sites facilitates the formation of neighbouring vacancies.

[1] Li et al., App Phys Lett 93, 072903 (2008)
[2] Mehonic et al., Adv Mat (2016), accepted for publication.
[3] Yao et al. Nano Lett 10, 4105 (2010).
[4] Mehonic et al., J of App Phys 111, 074507 (2012)
[5] Jin et al., Phys Rev Lett 86, 1793 (2001)

Amorphous carbon as a versatile semiconductor material for analytical electrochemistry

Miguel A. Caro and Tomi Laurila
Department of Electrical Engineering and Automation, Aalto University, Espoo, Finland

Amorphous carbon (a-C) and hybrid carbon nanomaterials integrated on an a-C matrix are emerging as a versatile material system for tailored electrochemical performance with targeted characteristics [2]. However, a-C properties are strongly influenced by the sp^2/sp^3 fraction and film thickness and morphology, and the observations are not always fully understood. Therefore, experimental results often need to be complemented with simulation in order to achieve a meaningful interpretation. We will present the results of density functional theory calculations to generate computational samples of a-C and simulate its electronic and structural properties [1]. We will show how the simulated properties affect the electrochemical performance of a-C electrodes and will discuss how experiment and simulation can (and should) go hand in hand in order to acquire a more in depth understanding of materials systems.

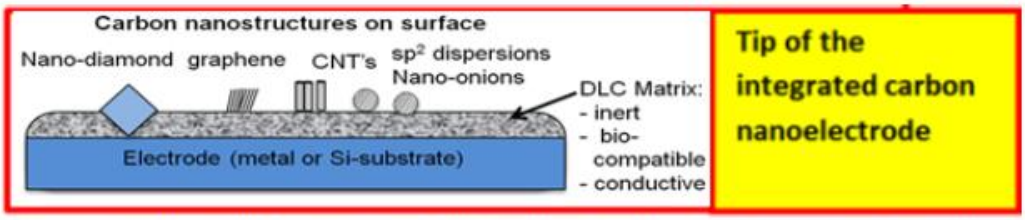

Illustration 1: Hybrid carbon materials offer excellent performance for in vivo electrochemical analysis

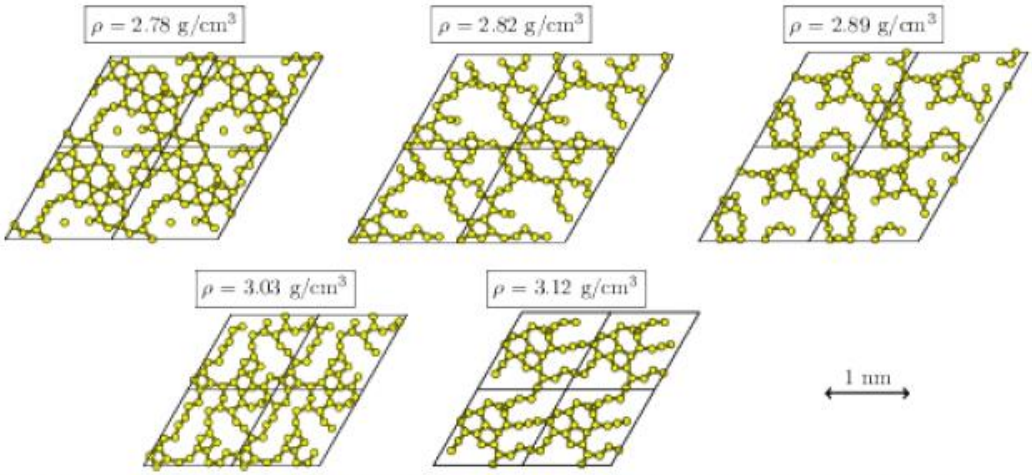

Illustration 2: Surface morphologies simulated for a-C samples of different densities

[1] M.A. Caro, R. Zoubkoff, O. Lopez-Acevedo and T. Laurila, Carbon 77, 1168 (2014)
[2] T. Laurila et al., Diamond and Related Materials 49, 62 (2014)

Making Correlated Systems More Tractable

Ben Hourahine
SUPA, Department of Physics, University of Strathclyde, John Anderson Building, 107 Rottenrow, Glasgow G4 0NG United Kingdom

This contribution will discuss methods for treating correlated systems in self-consistent tight binding methods, in particular the within the DFTB approach. Firstly the LDA+U[i] based methods available in the DFTB+ code[ii] will be reviewed, using lanthanide impurities in GaN and the thin-film topological insulator GdN as examples. I will then present first results for a 'DFTB+Gutzwiller' method which uses a novel way to couple the many body projection to the mean-field tight-binding. This approach has uses for 'reasonably correlated' systems, and is intended to be both faster than DMFT-based methods and more accurate than RPA-DFTB. This method may also offer a new way to treat delocalisation errors in DFTB, and hence DFT.

[i] B. Hourahine, S. Sanna, B. Aradi, C. Köhler, Th. Niehaus and Th. Frauenheim , *J. Phys. Chem. A* **2007** *111*, 5671-5677 DOI: 10.1021/jp070173b
[ii] B. Aradi, B. Hourahine, and Th. Frauenheim, *J. Phys. Chem. A* **2007** *111*, 5678-5684 DOI: 10.1021/jp070186p

Day 2

Session 4

Thursday, 8th December

16:30-17:45

New Materials

Modelling of the thermoelectric properties of materials near soft mode phase transitions

Ivana Savic
Tyndall National Institute, Cork, Ireland

Thermoelectric materials could play an important role in the development of energy harvesting technologies due to their ability to convert waste heat into electricity [1]. It is challenging to control and enhance the efficiency of thermoelectric energy conversion in a material because of the conflicting requirements for the desired physical properties i.e. high electrical conductivity and low thermal conductivity. Exploiting the fascinating properties of materials near soft mode phase transitions is an emerging concept in the quest to increase thermoelectric efficiency [2]. The underlying idea is that soft phonon modes lead to intrinsically low thermal conductivity, while possibly preserving high electronic conductivity.

In this talk I will focus on some of the unusual properties of PbTe, which is a classic thermoelectric material that exists near soft optical mode phase transition. I will briefly review the first principles approaches to calculate thermoelectric transport properties based on the Boltzmann transport equation [3,4], and discuss their application to PbTe based materials. Finally, I will present our predictions that driving PbTe closer to the phase transition via strain or alloying could substantially suppress its lattice thermal conductivity and possibly improve its thermoelectric efficiency [5].

[1] G. J. Snyder and E. S. Toberer, Nat. Mater. 7, 105 (2008).
[2] L.-D. Zhao et al, Nature 508, 373 (2014).
[3] D. A. Broido et al., Appl. Phys. Lett. 91, 231922 (2007).
[4] Z. Wang et al, Phys. Rev. B 83, 205208 (2011).
[5] R. M. Murphy et al, Phys. Rev. B 93, 104304 (2016).

Physical properties of the wide band gap II-IV nitride $MgSiN_2$

Mikael Råsander, James B. Quirk and Michelle A. Moram
Department of Materials, Imperial College London, United Kingdom

Ultraviolet light-emitting diodes (UV-LEDs) based on wurtzite structure III-nitrides currently have low efficiencies and lifetimes, since it is not possible to achieve lattice and polarisation matched quantum well heterostructures with appropriate band gaps and band offsets using either pure III-nitrides or their alloys. This motivates a search for alternative wide band gap nitride materials that could introduce additional degrees of freedom for UV-LED device design, either to assist in the lattice-matching or in the polarisation-matching within the active light-emitting region.

The Group II-IV nitride semiconductors are emerging as promising alternatives for these applications. These materials have wurtzite-derived orthorhombic crystal structures and can be obtained by substituting pairs of Group III (e.g. Al, Ga or In) atoms in a III-nitride for a single Group II (Be, Mg, Ca or Zn) atom and a single Group IV (C, Si, Ge or Sn) atom. We have focused on the II-IV nitride $MgSiN_2$ using both theory and experiment. On the theoretical side, density functional theory has been used to obtain accurate structural properties, elastic constants and piezoelectric properties of $MgSiN_2$. As an example, we have shown that $MgSiN_2$ has a large indirect band gap of similar size to the direct band gap of AlN, while having a crystal size which is intermediate between AlN and GaN.[1,2] $MgSiN_2$ should therefore facilitate better lattice matching during film growth compared to III-nitrides, and therefore constitutes a good candidate material to be used in novel high efficiency UV-LEDs. We have also studied the effects of adding Al to $MgSiN_2$, both when Al is added as an impurity as well as when added in larger concentration such that a quaternary Mg-Si-Al-N phase is formed.

[1] J. B. Quirk, M. Råsander, C. M. McGilvery, R. Palgrave and M. A. Moram, Appl Phys Lett 105, 112108 (2014)
[2] M. Råsander and M. A. Moram, Mater Res Express 3, 85902 (2016)

Surface plasmon resonance simulations in structures with chalcogenide layer

Laurentiu Baschir*), Aurelian A. Popescu, Dan Savastru and Sorin Miclos
National Institute R&D of Optoelectronics, INOE 2000, 409 Atomistilor str., PO BOX MG. 5, 77125 Magurele, Ilfov, Romania

*) baschirlaurentiu@inoe.ro

Chalcogenide materials have outstanding optical properties being very attractive for memory storage devices, fiber and integrated optics sensors, IR amplifiers and laser sources. However, the modification values of optical constants, the refractive index or absorption coefficient, are too small for practical applications. One of the way to improve the device characteristics is to place the amorphous chalcogenide films into structure with sharp resonance characteristics. The multilayer structure which employs surface plasmon resonance (SPR) may be very practical solution as it is sensible to very small, up to 10^{-6}, changes of refractive index.

In this paper we present several numerical simulations of the surface plasmon resonance in a metal-chalcogenide waveguide. We determined the thickness of the chalcogenide film for which plasmonic resonant coupling of the incident radiation to the waveguide occurs. We assume that the chalcogenide waveguide layer may have a finite thickness and operates as planar waveguide. The characteristic equation for four layer structure was obtained. Numerical simulations showed that for some thicknesses of the chalcogenide film the resonance conditions can be obtained using a low refractive index prism of BK7.

We calculated the electric and magnetic field distribution within the waveguide regions, the propagation constants, and evaluated the attenuation of different TE and TM modes. The dispersion equations were solved numerically by using a code implemented in MATLAB to determine the propagation constant as function of film thickness. These calculations permitted to determine the confinement within the waveguide layers. The obtained results provide the conditions for design optoelectronic devices based on light-light interaction in plasmonic configuration.

DNA sequencing using diamondoid-functionalized nanopores

Frank C. Maier, Ganesh Sivaraman, and Maria Fyta
Institute of Computational Physics, University of Stuttgart, Germany

Nanopores have been shown to be able to distinguish among the different DNA units, the nucleobases. In order to enhance the electronic tunnelling signals and reduce the errors in the read-out of the DNA nucleobases, functionalized nanopores have been proposed[1]. Previous work showed that DNA nucleobases show a specific binding to small diamond-like cages, the diamondoids, which is measurable[2]. Accordingly, modifying gold-electrodes with diamondoids which are placed within a nanopore can enhance the read-out properties of DNA molecules[3]. Here, we perform quantummechanical calculations within the density functional theory (DFT) approach together with the non-equilibrium Green's function (NEGF) formalism to further investigate the properties of functionalized nanopores. Specifically, we focus on double functionalized nanogaps and evaluate the electronic and quantum transport properties of various DNA units within the nanogaps. For this, the conductance across the nanopores and their sensitivity is assessed. The dynamics of the DNA, as well as the influence of a solvent will also be taken into account at a second step. In the end, we discuss the impact of our results on identifying DNA molecules through double functionalized nanopores.

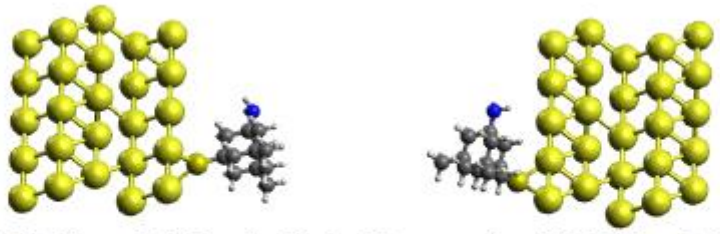

Figure 1: A double diamondoid-functionalized gold nanogap in which DNA nucleobases will be placed. The whole set-up is supposed to be inserted in a nanopore for sensing DNA.

[1] Branton, Daniel, et al., The potential and challenges of nanopore sequencing, Nature Biotechnology, 26, 1146-1153, 2008
[2] Maier, F. C. and Fyta, M., Type-Dependent Identification of DNA Nucleobases by Using Diamondoids, ChemPhysChem, 15, 3466–3475, 2014
[3] Ganesh Sivaraman, Rodrigo G Amorim, Ralph H Scheicher and Maria Fyta, Benchmark investigation of diamondoid-functionalized electrodes for nanopore DNA sequencing, Nanotechnology, 27, 10105-10112, 2016

Day 3

Session 1

Friday, 9th December

09:00-10:30

Hybrid Perovskites & Solar Cells

Unusual Optical Properties of MAPI

Mark van Schilfgaarde
King's College London, United Kingdom

Using the quasiparticle self-consistent GW approximation (QS*GW*) we analyse the electronic electronic structure and optical properties of MAPI ($CH_3NH_3PbI_3$) and related compounds. It is well known that density-functional theory (DFT) underestimates bandgaps; here we show that in MAPI, many electronic properties are poorly described, such as the valence band dispersions and Rashba splittings. We also show that quasiparticle self-consistency significantly further modifies the band structure relative to *GW*, based on DFT.

Spin orbit coupling modifies both valence band and conduction band dispersions in a very unusual manner: both get split at the R point into two extrema nearby. This can be interpreted in terms of a large Dresselhaus term, which vanishes at R but for small excursions about R varies linearly in *k*. Conduction bands (Pb 6*p* character) and valence bands (I 5*p*) are affected differently; moreover the splittings vary with the orientation of the moiety.

The crystal structure is ``pseudocubic", meaning that it is cubic on average. But the perovskite cage twists and flexes in time, causing the Rashba term to persist even in compounds such as $CsPbI_3$ without a symmetry-breaking moiety. This preserves the Rashba splitting; however, the band edges are not static, but rotate in time.

We carry out a QSGW based calculation of the photoluminescence in MAPI, and compare to available experimental data. We will show how the splittings, have important consequences for both electronic transport and the optical properties of this material.

If time permits we will also describe the possibility of MAPI as an intrinsic "photon ratchet" material with the potential to surmount the Schockley Quiesser limit.

Band gap engineering in perovskites as solar cell buffer layers

Matko Mužević, Igor Lukačević, Denis Stanić, Arijan Aleksić, Anja Novaković
Department of Physics, University of J.J. Strossmayer in Osijek, Croatia
Sanjeev Kumar Gupta
Department of Physics, St. Xavier College, Ahmedabad, India

Hybrid halide perovskites have recently attracted attention as materials for solar energy conversion. Devices' power conversion efficiency (PCE) has swiftly increased to over 19% during the past several years[1-4]. For this reason, they present the most promising candidate for the third generation solar cell. An indispensable part of solar cells is the buffer layer. Many inorganic perovskites (of structure XYO_3, X = Ca, Mg, Sr, Ba; Y = Mn, Tc, Re) have eminent photoelectric properties[5-8]. Because of their low price, nontoxicity, chemical and thermal stability and oxidation resistance in the air, we have simulated their electronic properties (using reliable quantum-mechanical calculations) for direct applications in solar cells based on hybrid halide perovskites. The best material for use in the solar cell buffer layer was identified by comparing the electronic band structure, HOMO and LUMO levels, with known levels of other hybrid halide perovskites, such as $CH_3NH_3PbI_3$.

[1] R. F. Service, Science 344, 458 (2014)
[2] J. H. Im, C. R. Lee, J. W. Lee, S. W. Park, and N. G. Park, Nanoscale 3, 4088 (2011)
[3] M. Liu, M. B. Johnston, and H. J. Snaith, Nature 501, 395 (2013)
[4] M. Grätzel, Nature Mater. 13, 838 (2014)
[5] P. Zhao, J. Xu, H. Wang, L. Wang, W. Kong, W. Ren, L. Bian, and A. Chang, J. Appl. Phys. 116, 194901 (2014).
[6] Y. Zang, D. Xie, X. Wu, Y. Chen, Y. Lin, M. Li, H. Tian, X. Li, Z. Li, H. Zhu, T. Ren, and D. Plant, Appl. Phys. Lett. 99, 132904 (2011)
[7] Y. Yuan, Z. Xiao, B. Yang, and J. Huang, J. Mater. Chem. A 2, 6027 (2014)
[8] M. A. Pen and J. L. G. Fierro, Chem. Rev. 101, 1981 (2001)

Computational challenges in the NEGF simulation of mesoscopic solar cell components

Urs Aeberhard,
IEK-5 Photovoltaik, Forschungszentrum Jülich, Germany

Many state-of-the-art solar cell architectures and most implementations of novel photovoltaic concepts include a set of functional nanostructure components, which results in the need of comprehensive multiscale approaches for the simulation-guided optimization of device performance. Since the functionality of the nanostructure components usually arise only in a device environment of mesoscopic extent, e.g., in the presence of doping-induced band bending or contacts, a quantum device model is helpful to mediate between the atomistic material simulation – often from first principles – and the macroscopic continuum device models on the semi-classical level. In this situation, the non-equilibrium Green's function formalism provides a powerful tool to obtain device characteristics at the nanoscale.

In our contribution, we discuss several computational challenges related to the application of the NEGF formalism to the simulation of nanostructure based solar cell devices [1], ranging from the parametrization of mesoscopic Hamiltonians of quantum dot arrays [2] to the convergence behaviour of the self-consistent Born approximation in the presence of localized states [3] and to efforts in the parallelization of an dedicated NEGF code for photovoltaic applications.

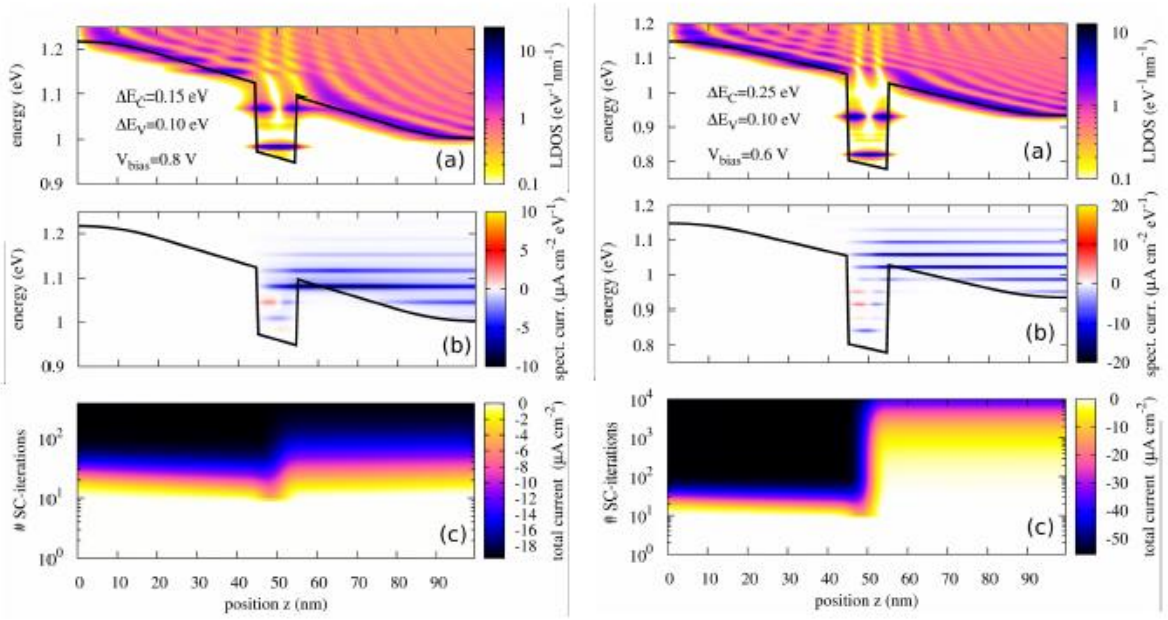

(a) Local density of electron states, (b) spectral electron current density and (c) convergence of the total current in the iteration process of the self-consistent Born approximation to electron-phonon and electron-photon self-energies, for an intermediate (left) and a deep (right) quantum well photodiode [3]. For the deep well, reaching a converged current in a reasonable time presents amounts to big challenge.

[1] U. Aeberhard, J. Comput. Electron. **10**, 394 (2011)
[2] A. Berbezier and U. Aeberhard, Phys. Rev. Appl. 4, 044008 (2015)
[3] U. Aeberhard, J. Comput. Electron. (online first), (2016).

Heuristic modeling of multi-junction solar cells

Slobodan Čičić and Stanko Tomić,
School of Computing, Science and Engineering, University of Salford, United Kingdom

In order to achieve the highest possible values of solar cell efficiencies, parameters, such as optimal energy gaps, thicknesses and impurity concentrations, have to be optimally selected. To find the optimal combination of these parameters, drift-diffusion model is used, with all material parameters calculated as a function of energy gap. This way we have very realistic material parameters which, together with detailed loss modeling, provide reliable results. Optimisation was conducted using genetic algorithm. As an example, in *fig 1* efficiencies for one-junction to five-junction solar cells are presented together with combination of optimal energy gaps determined in [1], where detailed balance method was used. Parameters which were optimised are thicknesses, impurity concentrations and optimal current. The optimisation was repeated in three different cases. First, with only radiative recombination taken into account. Next, radiative recombination and diffusion current. Finally, Auger recombination together with the other two. The optimised solar cell was not series constrained, which means optimal currents of individual cells in multi-junction solar cell are not equal. The result shows influence of each type of losses to overall efficiency. Progress of optimisation for four-junction solar cell is shown in *fig 2*. Diversity of results indicates there is small probability algorithm was in a local maximum. Calculations were carried out with ASTMG173 Global tilted spectrum and absorption calculated from kppw code [2]. To test the model, efficiencies were calculated with only radiative recombination and black body spectrum and compared with results from [1]. Results from both models are in agreement, which makes other results trustworthy.

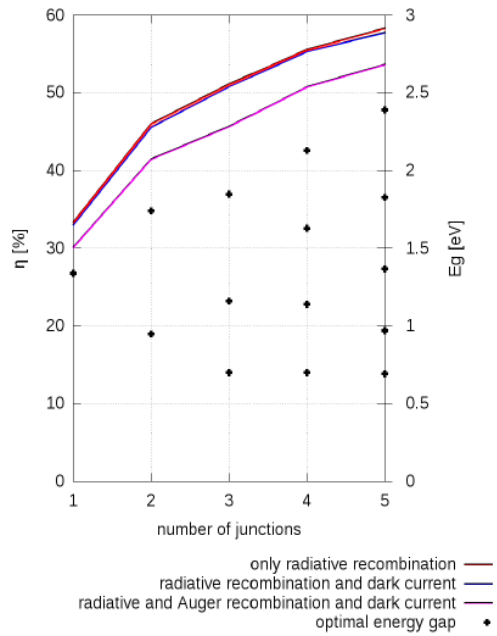

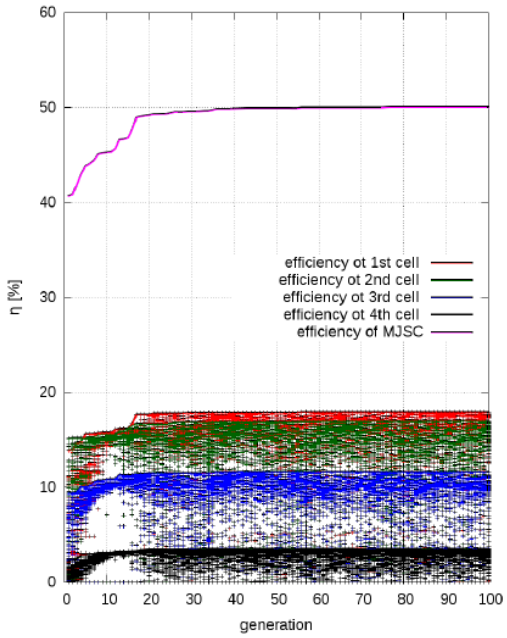

fig 1: Multi-junction solar cell elliciency *fig 2: Optimisation progress*

1. A.S. Brown, M.A. Green, "Detailed balance limit for the series constrained two terminal tandem solar cells", Physica E, Vol. 14, 96-100, 2002.
2. S. Tomic, A.G. Sunderland, I.J. Bush, "Parallel multi-band kp code for electronic structure of zinc blend semiconductor quantum dots", Journal of Materials Chemistry, Vol. 16, 1963-1972, 2006.

Optoelectronic properties of a-Si:H and a-Si:H/c-Si interfaces from first principles

Philippe Czaja and Urs Aeberhard
IEK-5 Photovoltaics, Forschungszentrum, Jülich, Germany
Massimo Celino and Simone Giusepponi, ENEA Casaccia, Italy

In order to optimize the optoelectronic properties of novel solar cell architectures, such as the amorphous-crystalline interface (a-Si:H/c-Si) in silicon heterojunction devices, we calculate and analyze the local microscopic structure at the interface and in bulk a-Si:H, and use the microscopic information for extracting macroscopic material properties.
In particular the impact of material inhomogeneities, such as structural defects and interfaces, on the electronic properties of a-Si:H and a-Si:H/c-Si structures, and on the optical properties of a-Si:H is investigated.
To this end, atomic configurations for a-Si:H consisting of 72 and 576 atoms respectively, and a-Si:H/c-Si interfaces consisting of 368 atoms are generated using Born-Oppenheimer molecular dynamics within the Quantum ESPRESSO[1] and the CP2K[2] code packages. Electronic structure calculations using DFT, as implemented in the PWscf code from the Quantum ESPRESSO suite, are then applied to these configurations in order to obtain the electronic wave functions and energies. These are analyzed and characterized with respect to their localization and their contribution to the (local) density of states.
For the small a-Si:H configuration, the results of both an independent-particle, and a quasi-particle corrected electronic structure calculation are used in calculating the spectral absorption coefficient from ab initio using the BerkeleyGW[3] code. The results suggest that the quasi-particle corrections in a-Si:H can be approximated by a scissors shift of the Kohn-Sham energies. The obtained scissors shift parameters are reused in absorption calculations for the bigger a-Si:H configuration.
Regarding the interface, the focus of interest is on the characterization of the wave functions with respect to their localization so as to identify localized defect states, which govern the recombination properties encoded in quantities such as capture cross sections used in the Shockley-Read-Hall theory.

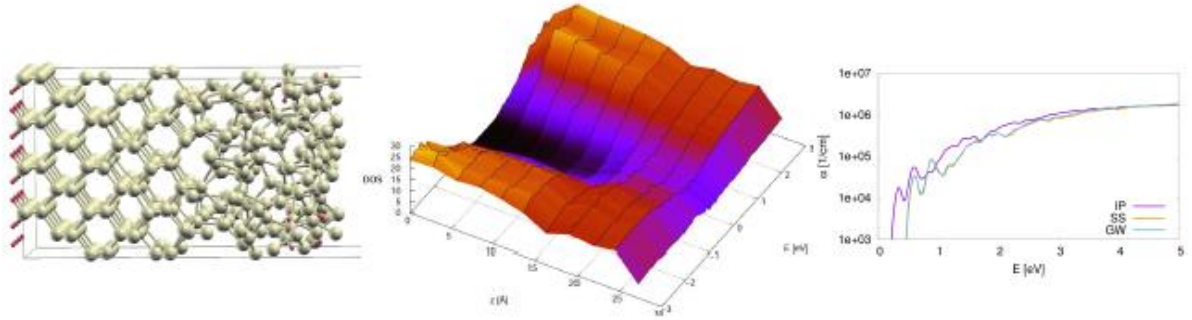

a-Si:H/c-Si interface configuration, layer-resolved density of states of the interface along the growth direction, and a-Si:H absorption spectrum at different levels of approximation

[1] P. Giannozzi et al., J. Phys. Cond. Mat. 21 (2009) 395502
[2] www.cp2k.org
[3] J. Deslippe et al., Comput. Phys. Commun. 183, (2012) 1269

Day 3

Session 2

Friday, 9th December

11:00-12:45

Device Simulations

Challenges in Optoelectric Device Simulation

Yuh-Renn Wu and Chi-kang Li
Graduate Institute of Photonics and Optoelectronics, National Taiwan University, Taipei, Taiwan
Marco Piccardo, Marcel Filoche, and Claude Weisbuch, Laboratoire de Physique de la Matière Condensée, Ecole Polytechnique, CNRS, Université Paris Saclay, 91128 Palaiseau Cedex, France

In recently years, modeling works on nitride based optoelectronics such as LEDs and laser diodes have face many challenges due to the existence of strong polarization field and random alloy potential fluctuations. Unlike arsenide based alloys, InGaN alloys have large bandoffsets potential fluctuations and much larger hole effective mass, where carriers expecially holes are strongly localized by the potential fluctuations. The existence of QW thickness fluctuations makes then analysis even more complicated. As we know, atomic based simulation models such as tight binding method[1] and DFT theory have been applied to study the effect of carrier localization and recombination, where the broadening of emission spectrum has been qualitatively explained. However, due to the computational burden, it is relatively impractical to apply these models to study the carrier transport throughout a full device structure, from contact regions to MQW active regions. While NEFG models might be good solution, modeling the whole device in MQW LEDs including all scattering mechanisms such as polar optical and accoustic phonon, impurities, radiative, nonradative, and Auger recombination is overwhelmingly time consuming and it is hard to get computational convergences. In our earlier work, we applied a 3D FEM based Poisson, drift-diffusion solver with strain analysis[2] to model the transport properties, where modeling results showed good prediction to the IV and IQE characteristic. However, the lack of including a quantum description of the carrier states missed some features especially on emission spectrum and some possible tunneling effects. Recently, we have worked on using the localization landscape theory[3] coupled with Poisson and drift-diffusion equations to model semiconductor devices and discussed how this model can be used in analyzing absorption Urbach tails due to the composition fluctuations. We also applied this model in finding the *effective* confining potential with quantum theory in modeling the carrier transport and recombination behavior in the InGaN MQW LEDs with compositional fluctuation effects included. The computational speed with this model has been reduced significantly compared to self-consistent Poisson-Schrodinger solver and a good prediction to LED I-V characteristics has been achieved. In this paper, we will discuss the issues we have faced and demonstrate how we approached these.

1. Schulz, S., et al., *Atomistic analysis of the impact of alloy and well-width fluctuations on the electronic and optical properties of InGaN/GaN quantum wells*. Physical Review B, 2015. **91**(3): p. 035439.
2. Yang, T.-J., et al., *The influence of random indium alloy fluctuations in indium gallium nitride quantum wells on the device behavior*. J. Appl. Phys., 2014. **116**(11): p. 113104.
3. Arnold, D.N., et al., *Effective Confining Potential of Quantum States in Disordered Media*. Physical Review Letters, 2016. **116**(5): p. 056602.

Effects of strain distribution on the emission properties of (In,Ga)N/GaN nanowire LEDs

Fabio Sacconi, Fabio Panetta
Tiberlab Srl , Rome, Italy
Mattia Musolino, Abbes Tahraoui, Lutz Geelhaar
Paul-Drude-Institut für Festkörperelektronik, Berlin, Germany
Carlo De Santi, Matteo Meneghini, and Enrico Zanoni, Department of Information Engineering, University of Padova, Padova, Italy

In this work we present a study of optoelectronic properties of (In,Ga)N/GaN nanowire (NW)-LEDs as a part of the validation task of the multiscale models developed in the framework of the project Deepen (FP7-NMP n.604416). Strain distribution, electronic structure, transport and optical properties of axial nanowire structures have been calculated and compared with experimental measurements performed on LEDs based on (In,Ga)N /GaN NW ensembles. The NW is composed of a MQW structure of four quantum disks (QD) with an In content of (25 ± 10) % and a nominal thickness of 3 nm, separated by 8nm-thick GaN barriers[1]. A parametric multiscale coupling has been implemented in simulations, consisting in employing parameters extracted from first-principle atomistic calculations in continuous media simulations. In particular, composition dependent values of band gap and conduction and valence band edges bowing parameters for (In,Ga)N alloy obtained from Empirical Tight-Binding (ETB) bulk calculations have been used.[2] 3D simulations have been performed with a drift-diffusion model including strain and polarization effects and with a 6x6 **k·p** model to yield eigenstates and optical spectra.[3] The results of these calculations show a very good agreement with the experimental behavior of the emission peaks (see Fig.1 and 2). Both peak energies and electroluminescence (EL) intensities are well reproduced by simulations, within an error due to uncertainties in the estimation of the average current density flowing in the single NW-LED. Moreover, a peculiar experimental evolution of EL peaks with increasing current in the NW is found, which results to be related to NW morphology and crystal polarity. It is found that this behavior is due to the particular strain pattern and relaxation effects present in the NW LED and not in a planar device. Through the study of 3D strain maps and quantum charge distribution inside the NW, we show how our simulation models may provide a deeper understanding of the emission properties of NW LEDs.

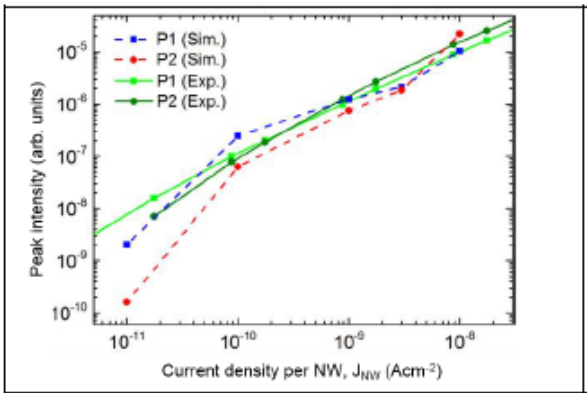

Fig.1 EL intensity in the NW LED for increasing current

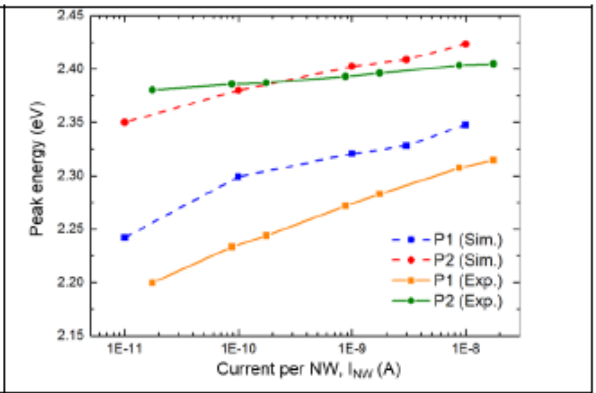

Fig.2 Peak emission energy in the NW LED for increasing current

[1] M. Musolino, A. Tahraoui, F. Limbach, J. Lähnemann, U. Jahn, O. Brandt, L. Geelhaar, and H. Riechert, Appl. Phys. Lett. 105, 083505 (2014)
[2] Miguel A. Caro, Stefan Schulz, and Eoin P. O'Reilly, PRB 88, 214103 (2013)
[3] M. Auf der Maur, G. Penazzi, G. Romano, F. Sacconi, A. Pecchia, and A. Di Carlo, Electron Devices, IEEE Transact. 58(5), 1425, (2011)

Christopher A. Broderick*, Wanshu Xiong and Judy M. Rorison
Department of Electrical and Electronic Engineering, University of Bristol, Bristol BS8 1UB, U.K.
***christopher.broderick@bristol.ac.uk**

Substitution of a small fraction of As by Bi in (In)GaAs brings about a strong decrease of the band gap (E_g) and increase of spin-orbit-splitting energy (Δ_{SO}). Theory and experiment confirm that Bi incorporation can bring about a band structure in which $\Delta_{SO} > E_g$, which should suppress non-radiative (Auger) recombination and inter-valence band absorption (IVBA) processes involving the spin-split-off band. These processes strongly limit the efficiency and performance of long-wavelength semiconductor lasers: their elimination promises to lead to the development of highly efficient devices with reduced temperature sensitivity, thereby facilitating the removal of the power-hungry external cooling required to maintain operational stability in existing devices[1].

Compared to the well-studied GaBiAs/GaAs material system, where Bi compositions $\gtrsim 10\%$ are required to achieve $\Delta_{SO} > E_g$, theoretical and experimental studies have demonstrated that a $\Delta_{SO} > E_g$ band structure can be achieved in InGaBiAs alloys grown on InP for Bi compositions as low as 4% [2]. Initial analysis has suggested that InGaBiAs alloys grown on InP are a promising material system for the development of highly efficient mid-infrared light-emitting devices[3], and epitaxial growth of alloys in which $\Delta_{SO} > E_g$ has recently been achieved[4].

In order to explore and quantify the potential of this material system for applications in the mid-infrared we have undertaken a theoretical investigation of InGaBiAs/InP quantum well (QW) laser structures designed to emit at wavelengths > 3 μm [5]. Through our analysis we identify several promising features of this material system including (i) the potential to greatly extend the emission wavelengths accessible to the InP platform (thereby opening up the application rich 3-5 μm spectral range), as well as the ability to (ii) exploit the impact of Bi to suppress the dominant Auger and IVBA loss mechanisms, and (iii) realise large type-I QW band offsets to mitigate carrier leakage at high temperature. In particular, the ability to grow diode lasers incorporating type-I QWs circumvents the requirement for metamorphic structures in order to facilitate long-wavelength emission on InP, and also removes the need to resort to complicated cascade structures, or non-ideal type-II QWs, which are often based upon the (compared to InP) expensive and technologically immature GaSb platform.

We present a comprehensive theoretical evaluation and optimisation of the performance of InGaBiAs/InP QW lasers designed to emit between 3 and 5 μm, and quantify important trends in the expected device properties as a function of alloy composition, strain, QW thickness and emission wavelength. On this basis we identify optimised structures that offer high performance and which are highly compatible with existing InP-based device architectures. Overall, our analysis highlights the strong promise of this emerging material system for mid-infrared photonics applications, and defines clear routes towards the realisation of optimised devices[5].

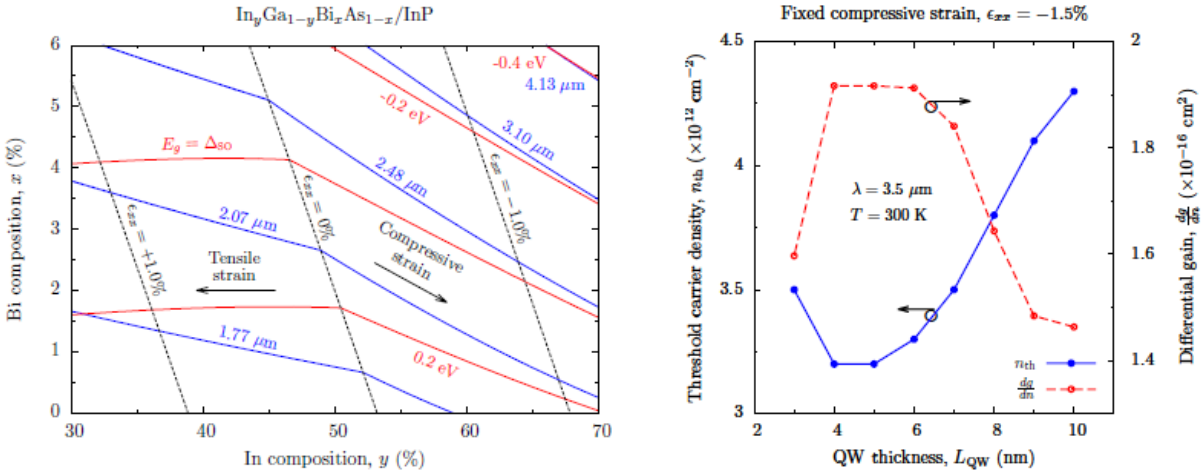

Figure 1: Left - Composition space map showing the variation of the strain (ε_{xx}; dashed black lines), band gap (E_g; solid blue lines), and difference between the band gap and spin-orbit-splitting energy (E_g - Δ_{SO}; solid red lines), for $In_yGa_{1-y}Bi_xAs_{1-x}$ alloys grown pseudomophically on InP. Right: - Variation of the room temperature sheet carrier density (n_{th}; closed blue circles) and differential gain (dg/dn; open red circles) at threshold as a function of QW thickness for a series of InGaBiAs QW laser structures designed to emit at 3.5 μm. The alloy composition for the InGaBiAs QWs in each structure was chosen to ensure that (i) the QWs are under 1.5% compressive strain, and (ii) their band structure has $\Delta_{SO} > E_g$ to facilitate Auger and IVBA suppression.

[1] C. A. Broderick, M. Usman, S. J. Sweeney, and E. P. O'Reilly, *Semicond. Sci. Technol.* **27**, 094011 (2012)
[2] C. A. Broderick, M. Usman, and E. P. O'Reilly, *Phys. Stat. Sol. B* **250**, 773 (2013)
[3] S. R. Jin and S. J. Sweeney, *J. Appl. Phys.* **114**, 213103 (2013)
[4] G. M. T. Chai, C. A. Broderick, E. P. O'Reilly, Z. Othaman, S. R. Jin et al., *Semicond. Sci. Technol*. **30**, 094015 (2015)
[5] C. A. Broderick et al., "*Theory of InP-based mid-infrared dilute bismide quantum well lasers*", submitted (2016)

Impact of short range Coulomb repulsion on the current through a 1D Nanostructure

Antonio Martinez[1], John R Barker[2] and Riccardo Di Pietro[3]
[1]College of Engineering, Swansea University, UK
[2]University of Glasgow, UK
[3]Hitachi Cambridge Laboratory, Cambridge, UK

In this work we present a methodology describing Coulomb blockade into the Non Equilibrium Green Function formalism (NEGF)[1], which is based on the incorporation of the two-particle Green function (2pGF). Previous work[2] using the 2pGF in conjunction with NEGF assumed the central region of the nanostructure or the quantum dot as featureless and only describes it using the energy level and coupling constants. In standard NEGF, the potential energy on the electron is calculated in the mean field approximation. The 2pGF[2] incorporates the short-range electron-electron interaction[3]. Using a toy model structure we have carried out ballistic and dissipative (phonon scattering) calculations of the current. An increase of current is demonstrated. This is due to the shift and splitting of the energy levels caused by electron repulsion inside the structure. Fig. 1 shows the local density of states (LDOS) with and without considering the 2pGF. The short-range Coulomb energy is 100 meV.
When the 2pGF is neglected, the ground state energy of the structure is lower than the source potential energy. In addition the next confined state energy is too high in energy to influence the current. In the upper panel the 2pGF is considered and as a consequence the ground state energy is lifted over the source potential entering into the bias bandwidth. This substantially enhances the current by more than 100% as shown in Fig. 2. Phonon scattering reduces the current substantially when the 2p-GF is included. The method developed here can be extended to describe recent results[4] on charge transport in polymer semiconductors, where the presence of crystalline and amorphous domains leads to a confinement of charge carriers in nanometer scale crystallites[5].

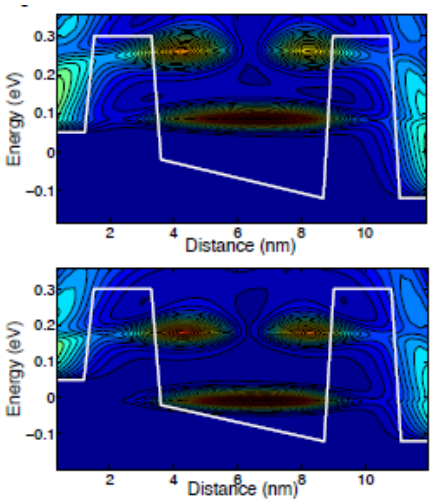

Fig.1 Upper panel: The LDOS including 2pGF. Lower panel: The LDOS without considering the 2pGF

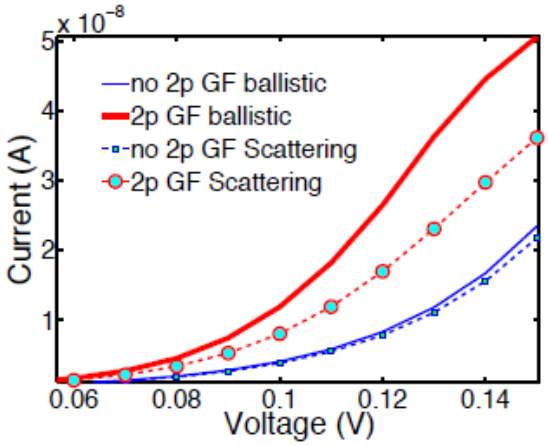

Fig.2 The current voltage characteristics for ballistic scattering simulations. The simulations showed in red, in the 2pGF and the blue neglected it.

[1] A. Svizhenko et al, J. Appl. Phys. 91, 2343 (2002).
[2]B. Song et al, Phys. Rev. B 76, 155430 (2007)
[3] J. Hubbard, Proc.Roy.Soc. A 276, 238 (1963),
[4]Di Pietro et al, Adv. Funct. Mater. Accepted for publication (2016)
[5]R. Noriega, et al, Nature Materials 12, 1038 (2013)

Effect of alloy and dopant scattering in $In_{1-x}Ga_xAs$ nanowires

Pedram Razavi and Jim Greer
Tyndall National Institute, University College Cork, Ireland

The effect of dopant and alloy scattering in $In_{1-x}Ga_xAs$ ultra-narrow nanowires (NWs) using density functional theory (DFT) in conjunction with a Green's function scattering methods is studied. It is known that scattering mechanisms have an increasing impact on limiting charge carrier mobility as the NW critical dimensions are reduced. For extremely short NW lengths for which transport is in the ballistic regime, surface and dopant scattering can dominate charge transport. A principle cell constructed from two unit cells are used for the atomic description of the NW. The NWs are of approximately square cross section and are approximately 1.1×1.1 nm^2 as shown in figure 1. These dimensions represent effectively the atomic scale limit for crystalline $In_{1-x}Ga_xAs$ NWs. Ideal surface passivation is accomplished using 'pseudo-hydrogen' atoms which are fictitious atoms with fractional charge of 0.75 and 1.25 and are used to chemically saturate the surface dangling bonds in III-V materials arising from the different valence of the group III and group V atoms at the surface of the NW. The chemically saturated NWs remain semiconducting and no defect states associated with the non-ideal surface passivation appear in the band gap of the NW. Band structures, density of states (DOS), and transmission for <100>-oriented $In_{1-x}Ga_xAs$ nanowires are presented, where by changing the composition from $x = 0$ to 1 in steps of 0.25, the effect of alloy composition on the band structure of $In_{1-x}Ga_xAs$ nanowires is extracted. Through the introduction of different dopants species at the surface and within the core of the $In_{1-x}Ga_xAs$ nanowires, the influence of dopant type and its position on charge transmission is investigated. The results allow for a qualitative assessment of the impact of specific scattering mechanisms within the NWs and can be directly related to the electrical performance of $In_{1-x}Ga_xAs$ nanowires near atomic scale limits.

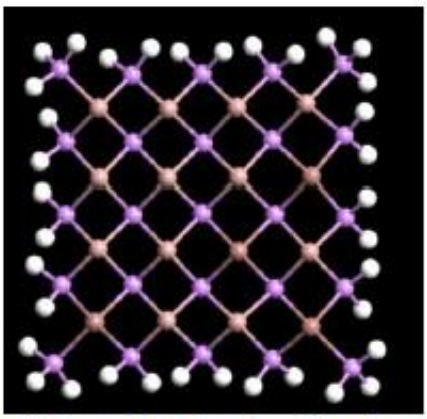

Figure 1. Schematic of an $In_{25}Ga_{75}As$ nanowire.

Acknowledgment: This work was supported by the European Union 7th Framework Programme DEEPEN (grant agreement no.: 604416).

Multi-scale modelling and simulation of single-photon sources on a device level

Markus Kantner, Uwe Bandelow, Thomas Koprucki and Hans-Jürgen Wünsche
Weierstrass Institute for Applied Analysis and Stochastics, Germany

Single-photon sources (SPSs) are key components for many applications in quantum cryptography and optical quantum computing. Semiconductor quantum dots (QDs) are excellent candidates for the realization of SPSs since they show a discrete energy spectrum, narrow line width and can be fabricated within micro-cavities.

Using numerical simulation of carrier transport, the current paths of electrons and holes can be investigated. Typically, SPSs are operated at low injection currents (few nA) and cryogenic temperatures. To achieve efficient current injection into the QD in this regime, a specific device design is necessary.[1] However, the computation of quantum optical quantities, such as the single-photon emission rate and the second order correlation function, requires a quantum mechanical description of the QD, which is beyond the scope of standard simulation tools.

We present a multi-scale model for electrically driven SPSs, based on the self-consistent coupling of a semi-classical transport model to a quantum master equation. The latter describes the QD as an open quantum system, which is embedded in the surrounding device.

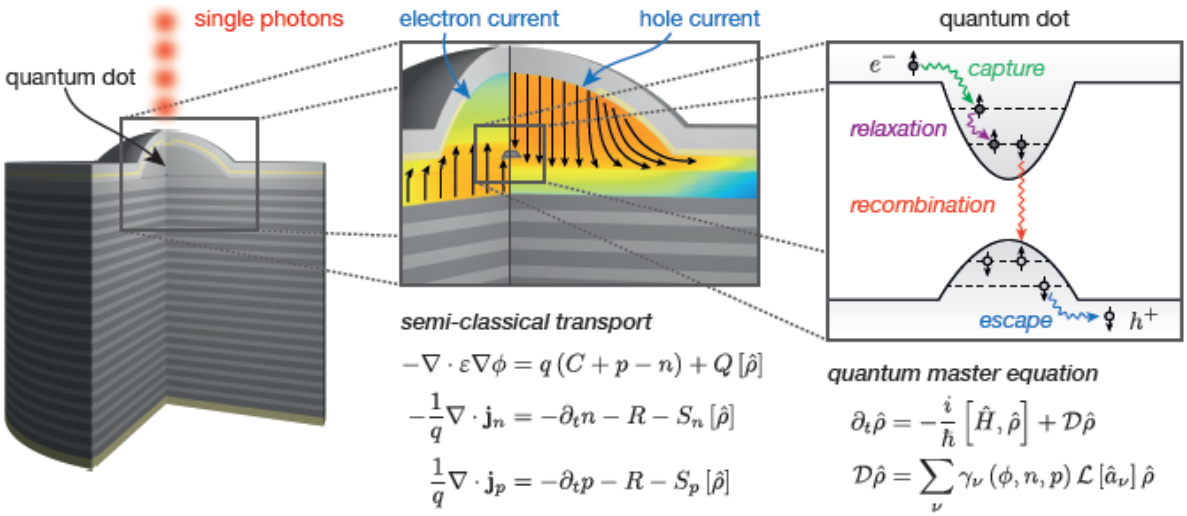

Fig. 1: **Schematic representation of the modelling approach.**

Our model provides a multi-species description of the charge carriers confined in the QD, the wetting layer (WL) and the freely roaming bulk carriers. On a microscopic scale, we start with a many-body Hamiltonian including electron-phonon, electron-photon and electronelectron interactions. Following Lindblad's approach[2], we derive a quantum master equation describing the QD carrier dynamics. The scattering rates are obtained as functions of the WL and bulk carrier densities and provide the link to the macroscopic transport model. The latter one is an extended multi-species drift-diffusion model, describing the transport of WL and bulk carriers.[3] Particular challenges arise from the cryogenic operation temperatures, which lead to a strong degeneration of the electron-hole-plasma and considerable numerical issues.[4] We demonstrate our approach by simulations of a specific device.

[1] M. Kantner *et al.*, *IEEE Trans. Electron Dev.* **63**(5), 2036−2042 (2016)
[2] H.-P. Breuer and F. Petruccione, *Theory of Open Quantum Systems*, Oxford University Press (2007)
[3] S. Steiger, R. Veprek, and B. Witzigmann, *J. Comput. Electron.* **7**, 509−520 (2008)
[4] M. Kantner and T. Koprucki, *WIAS Preprint* 2296 (2016), submitted to *Opt. Quant. Electron.*